Rossby solitons (Experimental investigations and laboratory model of natural vortices of the Jovian Great Red Spot type)

M. V. Nezlin

I. V. Kurchatov Institute of Atomic Energy

Usp. Fiz. Nauk **150**, 3–60 (September 1986)

This review is devoted to a new object in nonlinear physics—Rossby solitons. The following questions are examined in greatest detail: 1) experimental observation of Rossby solitons in the laboratory; the geometric and kinematic properties, stability, collisions, and methods of generation of Rossby solitons; 2) self-organization of a Rossby autosoliton in unstable oppositely directed (zonal) flows; 3) a stationary laboratory model of natural vortices of the Jovian Great Red Spot (JGRS) type based on the Rossby autosoliton; 4) the question of the uniqueness of the JGRS along the perimeter of the planet; and 5) paired Rossby vortices. The theory and experiment are compared. The analogy between Rossby vortices and drift vortices in a plasma is pointed out.

CONTENTS

 0038-5670/86/090807-36$01.80

INTRODUCTION

This review is concerned with structures which appear to be vortices on the one hand and solitary waves or solitons on the other. Their vortex properties are determined by the Coriolis force, associated with the global rotation of the medium in which they exist, while the soliton properties are associated with the equilibrium between dispersion and nonlinearity. These dualistic structures can be called both vortex solitons and wave vortices. As waves they belong to the branch of Rossby drift waves, which exist in the oceans and in planetary atmospheres; the frequencies of these waves are much lower than the global rotational frequency of the planet, while the wavelengths can be of a planetary scale—they are much larger than the depth of the ocean or the atmosphere. When their amplitude is large these waves transform into planetary vortices. The largest of these vortices is called the Jovian Great Red Spot (JGRS).[1)] This atmospheric vortex, which is significantly larger than the earth, has been observed for 300 years. Apparently, synoptic vortices in the earth's oceans and also stationary planetary vortices (so-called blockings[5]), which could be responsible for prolonged droughts on earth, have the same structure. With respect to such long structures the atmosphere or the ocean is a quasi-two-dimensional medium and can be rgarded as "shallow water." This, as well as the comparatively slow rotation, is what fundamentally distinguishes them from cyclones, whose intrinsic rotational frequency, on the contrary, is much higher than the global rotational frequency of the planet. (To better distinguish waterspouts and hurricanes from the planetary vortices studied in this review and their models in laboratory experiments in shallow water we recommend to the reader Refs. 1–5.)

Planetary waves (vortices) are named after the Swedish geophysicist Rossby, who showed that they play an important role in global atmospheric circulation processes.[7,2)] They can be successfully simulated in the laboratory.[9,11–17] The theory of planetary waves is reviewed in Refs. 23–27, blockings are studied in Refs. 18, 10b, and 44, and synoptic vortices in the oceans are studied in Refs. 19 and 20. Rossby waves are physically analogous to drift waves in a spatially nonuniform magnetized plasma. It is possible that they are linked with the generation of magnetic fields in nature.[21,22]

Rossby solitons are solitary planetary waves or nonspreading nonlinear Rossby wave packets, in which the dispersion spreading (characteristic of a linear wave packet) is balanced by nonlinear self-compression, and the wave propagates without a change in shape. The term "soliton" is sometimes applied only to such a solitary wave, which emerges unchanged in collisions with a similar wave (see, for example, Refs. 28–29). This definition is widely used primarily by mathematicians. Physicists, however, usually define a soliton as a solitary wave, irrespective of the results of mutual collisions of such waves (see, for example, Refs. 32–35). We shall do so also. Until recently Rossby solitons were studied only theoretically, and there are many reviews of this work[19a,39a] (see Refs. 30 and 31 for the early work on the theory of solitons in plasmas). This review is devoted to *experimental investigations* of Rossby solitons, which were initiated after solitons were observed in the laboratory at the beginning of 1981. The basic results of the theory are presented, and compared with experiment.

Experiments with Rossby solitons have passed through several stages. In the first stage the Rossby soliton was regarded as a non-steady-state vortex, produced by the short-time action of a generator, existing without spreading significantly longer than a linear wave packet and decaying gradually owing to viscous losses of momentum. In the second stage, steady-state structures—chains of Rossby solitons, generated by unstable, oppositely moving, zonal flows—were obtained. In the third stage, a self-organized and self-maintained steady-state anticyclonic *solitary* vortex—a Rossby autosoliton—was generated in a system of flows. This structure can be regarded as a physical, experimental model of the Jovian Great Red Spot,[36–38] constructed by the method of physical, analog simulation in shallow water.[3)] This method is based on the analogy between the equations of two-dimensional gas dynamics and the equations of shallow-water dynamics.[101] Analog physical simulation has substantial advantages over standard computer simulation, one of which is the simplicity of the experimental implementation. The illustration of the advantages of this method—using as examples the simulation of planetary vortices—is the main goal of this review. (See Ref. 40 for a discussion of the analog physical simulation of phenomena on a cosmic scale.)

1. ROSSBY WAVES

1.1. Conditions of existence and nature

Rossby waves arise in the atmosphere or in the ocean on a rotating planet and are distinguished by their low frequencies (ω) and long wavelengths (λ), namely, $\omega \ll \Omega_0$ and $\lambda \gg H$ (the "shallow water condition) where Ω_0 is the angular rotational frequency of the planet and H is the effective depth of the planet's atmosphere (ocean). The conditions for the existence of these waves can be easily determined with the help of Euler's equation:

$$\frac{\partial \mathbf{v}}{\partial t} + (\mathbf{v}\nabla)\,\mathbf{v} + 2\,[\boldsymbol{\Omega}_0 \mathbf{v}] = -\frac{1}{\rho}\nabla p. \qquad (1)$$

Since $\partial v/\partial t \approx \omega v$ and $(\mathbf{v}\nabla)\mathbf{v} \approx \omega v$, the first two terms on the left side of (1) are much smaller than the third term, and (1) assumes the form of the equation of geostrophic equilibrium:

$$2[\Omega_0 \mathbf{v}] = -\frac{1}{\rho}\nabla p \tag{2}$$

—the Coriolis force is balanced by the hydrostatic pressure gradient $p = \rho g^* H$, where ρ is the density of the medium and g^* is the acceleration due to the resultant of the gravitational force and the centrifugal force from the global rotation. The ratio of the centrifugal force from the rotation of a particle in the wave to the Coriolis force is called the Rossby number, Ro. In the regime under study (called the Rossby regime) we have

$$\mathrm{Ro} = \left|\frac{(\mathbf{v}\nabla)\,\mathbf{v}}{2\Omega_0 v}\right| \approx \frac{v}{L\Omega_0} \approx \frac{\omega}{\Omega_0} \ll 1. \tag{3}$$

Thus under the conditions of existence of Rossby waves the Coriolis force plays the decisive role. Rossby waves arise as a result of the spatial nonuniformity of this force, associated with the dependence of the local vertical component Ω_{0z} of the angular rotational velocity vector Ω_0 of the system on the latitude (φ), namely, $\Omega_{0z} = \Omega_0 \cos\alpha$, where $\alpha = \pi/2 - \varphi$. Rossby waves propagate westward, opposite to the global rotation of the planet. This propagation is a drift motion, occurring perpendicular to both the direction of the angular rotational velocity vector of the planet Ω_0 and the direction of the gradient of the Coriolis parameter

$$f = 2\,\Omega_0 \cos\alpha. \tag{4}$$

The mechanism of this drift[26b] is essentially analogous to the mechanism of the drift of charged particles in a nonuniform magnetic field "crossed" with its own gradient.[82]

1.2. Dispersion

The dispersion equation for Rossby waves can be easily obtained with the help of the standard procedure. From the equation of motion (1) and the equation of continuity for a liquid with a free surface

$$\frac{\partial H}{\partial t} + \operatorname{div}(H\mathbf{v}) = 0 \tag{5}$$

one easily obtains a solution whose expansion in a series in powers of the Rossby number (3), followed by linearization, yields an equation for the frequency ω and the phase velocity v_P of Rossby waves with arbitrary wavelength $\lambda = 2\pi/k$[23,24]:

$$\omega = -\frac{k_x \beta}{k_x^2 + k_y^2 + r_R^{-2}}, \tag{6}$$

$$v_\Phi = \frac{\omega}{k_x} = -\frac{\beta r_R^2}{k^2 r_R^2 + 1}, \tag{7}$$

where $k^2 = k_x^2 + k_y^2$; k_x and k_y are the wave numbers corresponding to oscillations along the parallel and along the meridian; x is the coordinate along the parallel (the eastward direction being positive) and y is the coordinate along the meridian (the northward direction being positive); $\partial/\partial y = (1/R)\partial/\partial\varphi$, R is the radius of curvature of the system (radius of the planet);

$$r_R = f^{-1}(g^* H)^{1/2} \tag{8}$$

is the characteristic size of the dispersion or the Rossby-Obukhov radius; and, H is the equivalent depth of the medium. In the case of an atmosphere consisting of molecules with mass M and temperature T[4)]

$$H = kT/Mg^*, \tag{9}$$

$$r_R = c_S/f, \tag{10}$$

where $c_s = (kT/M)^{1/2}$ is the isothermal velocity of sound. We shall present several examples. For the earth $H \approx 8$ km and $r_R \approx 3000$ km; for Jupiter $H \approx 25$ km and $r_R \approx 6000$ km; and, for Saturn $H \approx 80$ km and $r_R \approx 6000$ km.

The parameter β appearing in (6) and (7) is determined by the relation

$$\beta = -\frac{f^2}{H}\frac{\partial H/f}{\partial y}, \tag{11}$$

or

$$\beta = \frac{\partial f}{\partial y} - \frac{f}{H}\frac{\partial H}{\partial y}. \tag{11'}$$

It is evident from (11) that a Rossby wave arises as a result of the meridional nonuniformity of the Coriolis parameter or depth of the liquid. This phenomenon is called the β effect. The direction of propagation of the wave is determined by the sign of the expression (11). In particular, for $H = \text{const}$, which occurs, for example, in a planetary atmosphere or ocean of uniform depth,

$$\beta = \frac{\partial f}{\partial y}. \tag{11''}$$

The phase velocity of Rossby waves for $H = \text{const}$ is oriented westward ["minus" sign in (6) and (7)]. Under other conditions, namely, in the presence of a quite large northward gradient of the thickness H of the layer of liquid, the phase velocity of Rossby waves, as is evident from (11), can in principle also be directed eastward. Although this situation occurs on planets only in the presence of a quite strong wind (see Sec. 1.4), it can be realized without difficulty experimentally (see Sec. 3.1.4).

The velocity of the waves depends on their wavelength, $\lambda = 2\pi/k$. For the longest waves ($k \to 0$) the phase velocity approaches the limit—the so-called Rossby velocity

$$V_R = |\beta|\, r_R^2. \tag{12}$$

In the particular case $H = \text{const}$, according to (11''),

$$V_R = r_R^2 \frac{\partial f}{\partial y}. \tag{12'}$$

It is important to note a different approximation, which is practically always used in the theoretical analysis of Rossby waves. This is the so-called β-plane approximation: the waves propagate not on the spherical surface of the planet, but rather (in order to simplify the analysis) on the tangent plane to this surface. In this approximation the Coriolis parameter is given by

$$f = f_0 + \frac{\partial f}{\partial y} y = f_0 + \beta y, \tag{4'}$$

where y is the northward displacement in the β plane from the point under study, and in addition β is assumed to be independent of y; corresponding to (4')

$$\beta = -\frac{1}{R}\frac{\partial f}{\partial \alpha},$$

where R is the radius of curvature of the meridian of the planet.

1.3. Nonlinearity of Rossby waves: scalar and vector

According to Oertel's theorem[23-25] about the conservation ("frozen-in" nature) of a potential vortex in shallow water

$$\frac{\mathrm{d}}{\mathrm{d}t}\left(\frac{\mathrm{rot}\,\mathbf{v}+\mathbf{f}}{H}\right)_z=0,$$

where the first term in the numerator is the local vorticity of the liquid, $f=2\Omega_0$ is twice the projection of the angular velocity vector of the system on the local vertical, $H=H_0+\delta H$ and δH is the perturbation of the surface of the liquid ($h=\delta H/H_0\ll 1$). In the case of two-dimensional motion studied here, one can introduce the stream function ψ, whose derivatives $(-\partial\psi/\partial y, \partial\psi/\partial x)$ determine the components of the velocity of the liquid along the parallel and along the meridian. Under the conditions of geostrophic equilibrium (2) and (3) we have $\delta H=(f/g)\psi$. Expanding $[1+(\delta H/H_0)]^{-1}$ in a series and omitting terms of order higher than second order, from Oertel's theorem we obtain

$$(\Delta\psi-r_R^{-2}\psi)_t-\beta k_x\psi+A(\psi^2)_x+BJ(\Delta\psi,\psi)=0, \quad (13)$$

where $J(\Delta\psi,\psi)=\Delta\psi_x\psi_y-\Delta\psi_y\psi_x$ is the Jacobian; the subscripts denote differentiation with respect to x (along the parallel) and y (along the meridian) in units of a and with respect to t in units of R/v_R; A and B are coefficients associated with the parameters of the system, such as Ω_0,β,R,r_R. It is assumed that β is independent of y ($\beta=\mathrm{const}$). The first two terms in Eq. (13) determine the dispersion of Rossby waves. Indeed, making the substitution $\psi_t\to\omega\psi$, $\Delta\psi=-k^2\psi$, in the linear approximation we obtain from (13) the dispersion equation (6). The third and fourth terms in (13) account for the two nonlinearities of Rossby waves: scalar and vector, respectively. The scalar nonlinearity[43] is related directly to the change in the thickness H of the layer of liquid. It is usually included in equations for nonlinear waves, for example, in the Korteweig–de Vries (KdV) equation,[3a,32] whence follows the *positive-elevation soliton* on shallow water—the first soliton in the history of science, observed by Scott Russell 150 years ago.[28b,d] The vector nonlinearity need not be associated with the variation of H. These nonlinearities can be separated strictly speaking only in asymptotic model situations. Thus the scalar nonlinearity vanishes when the liquid does not have a free surface, while the vector nonlinearity does not occur when the following two conditions are satisfied simultaneously: the vortex is axially symmetric and the Rossby velocity is constant in space.[142] Taking the ratio of the third term to the fourth term we obtain the following conventional estimate of the quantitative relation of these nonlinearities[42]:

$$\frac{\text{Scalar nonlinearity}}{\text{Vector nonlinearity}}\approx\frac{a^2}{r_R^2}. \quad (14)$$

Therefore when

$$a>r_R \quad (15a)$$

the scalar nonlinearity predominates, while when

$$a<r_R \quad (15b)$$

the vector nonlinearity predominates. These rough relations are of an evaluative nature and (as will become obvious from the discussion in Sec. 8) are useful for the experimental search for conditions under which one or the other nonlinearity may be expected to predominate.

The asymmetry of the nonlinear properties of cyclones and anticyclones (we recall that in cyclones and anticyclones the vorticity is oriented parallel and antiparallel, respectively, to the vector Ω_{0z}) follows from Eq. (13). Indeed, it is evident from the equation of geostrophic equilibrium (2) that for a cyclone $h<0$, while for an anticyclone $h>0$. When the cyclone is replaced by an anticyclone the signs of all terms in Eq. (13), except for the third one, are reversed, while the sign of the third term remains unchanged. This sign is such that, as is easily seen, the scalar nonlinearity can balance dispersion (i.e., cause an effect opposite to that of dispersion) only in the case of an anticyclone.[42] For a cyclone, however, the dispersion and scalar nonlinearity have the same signs and, therefore, cannot mutually compensate one another. This implies that if there exists a "scalar" Rossby soliton (a solitary wave in which the dispersion spreading is compensated by the twisting produced by the scalar nonlinearity), then it can only be an anticyclone, i.e., only a positive-elevation soliton, as in the case of the classical Russell soliton mentioned above. This cyclone-anticyclone asymmetry, as we shall see below, largely determines the possibility (or impossibility) of the formation of solitary vortices with different polarity (see Secs. 3, 4, 5, 8 and Ref. 42).

It will be shown below that planetary vortices of the Jovian Great Red Spot (JGRS) type occurring in nature as well as solitary (monopolar) Rossby vortices observed in the experiments studied in this review satisfy the relation (15a). Therefore when we talk about vortices we refer to a model which does not ignore the scalar nonlinearity, i.e., it is constructed based on taking into account both types of nonlinearities, as done, for example, in Ref. 42. The fundamental deficiency of the first soliton model of the JGRS (see Sec. 2.2) is that the scalar nonlinearity is ignored. Under the conditions of existence of dipolar vortices (see Sec. 8), however, the vector nonlinearity can predominate—in accordance with the relations (14), (15a), and (15b).

An important variant of the vector nonlinearity is studied in theoretical papers of Ref. 39. It occurs in the presence of a gradient of the magnitude of the Rossby velocity along the meridional coordinate y [when $\beta\neq\mathrm{const}$ in Eq. (13)]. This gradient can be due to the variation of any of the parameters appearing in the expressions (11) and (12) along the y axis. The nonlinearity associated with the dependence $H(y)$ and the so-called topographic Rossby solitons generated by it are studied specifically in Ref. 39. This nonlinearity can appear in planetary atmospheres and in the oceans; another case in which it can appear is mentioned in Sec. 6.

1.4. Manifestation of Rossby waves on earth

Among the manifestations of Rossby waves on our planet we shall study first of all the most interesting one from the viewpoint of this review—synoptic vortices in the oceans discovered by Soviet researchers.[19] In the interpretation of these vortices it is necessary to take into account the nonuniformity of the density of the ocean along the vertical coordinate (owing to the dependence of the density on the temperature, pressure, and salinity). But this nonuniformity, as it turns out,[19,26] makes it necessary to take into account the wave motion not only along the horizontal direction (as done above), but also along the vertical direction. Taking into account the vertical wave motion in Rossby waves leads to an interesting result: the dispersion equation for the waves remains structurally identical, but the characteristic size of the dispersion is now no longer the Rossby-Obukhov radius (8) (it is called barotropic), but rather the so-called internal (or baroclinic) Rossby radius:

$$r_1 = \frac{NH}{m\pi f_0}, \tag{16}$$

where N is the Brunt-Väisälä frequency of the vertical oscillations of a nonuniform liquid, which is stable with respect to convection (the density of the liquid ρ decreases in the vertical direction). In an incompressible medium

$$N = \left(-\frac{g}{\rho}\frac{\partial \rho}{\partial z}\right)^{1/2}; \tag{17}$$

compressibility leads to the appearance in the parentheses in (17) of a second term, equal to g^2/c_s^2, where c_s is the velocity of sound in the medium; m is the number of the vertical mode in the top layer of the ocean. Under the conditions prevalent in the ocean, for $m = 1$, the quantity $r_i \approx 50$ km (much smaller than the quantity $r_R \approx 2000$ km) is very close to the dimensions of the synoptic vortices observed, while their drift velocity (westward), which is of the order of several cm/s, approximately corresponds to the Rossby velocity βr_i^2 (but certainly not to βr_R^2, which would correspond to a vertically uniform medium). For this reason synoptic vortices in the oceans are regarded[26] as baroclinic Rossby waves. They fit into the ocean precisely because their dimensions are determined by the quantity $r_i \approx 50$ km, and not by the quantity $r_R \approx 2000$ km. Another example of an analogous rule is the natural atmospheric vortex in the Jovian Great Red Spot (see Sec. 2.2) and deep (internal baroclinic) anticyclonic vortices ("lenses") with dimensions $\sim r_i$ in the oceans on earth (see Sec. 5.2).

We shall now study the important question of the formation of a standing planetary vortex formed as a result of the stopping of a Rossby wave by wind blowing in the opposite direction.[18,24,44] Assume that the Rossby wave propagates in a medium which itself moves relative to the planet with a velocity u (the positive direction of this velocity is eastward). If the atmosphere is uniform in a motionless medium (i.e., no wind), then the wind makes it nonuniform: the Coriolis force, proportional to fu, which gives rise to a hydrostatic pressure gradient balancing it [see (2)], acts on the wind:

$$g\frac{\partial H}{\partial y} = -fu.$$

Now the velocity of the Rossby wave relative to the wind is determined by the relations (6) and (11), while the velocity of the wave relative to the planet equals

$$V = \frac{\omega}{k_x} + u = \frac{(uk^2 - \partial f/\partial y)\, r_R^2}{1 + k^2 r_R^2}.$$

It is evident that if the wind velocity satisfies the condition

$$u = \frac{1}{k^2}\frac{\partial f}{\partial y},$$

then the Rossby wave, propagating westward in the absence of the wind, is stopped by the oppositely blowing wind. Under terrestrial conditions this equality for the wavelength $\lambda = 2\pi/k \approx 3000$ km can be established with a wind velocity of several m/sec. We shall now take into account the fact that a Rossby wave with a sufficiently large amplitude exhibits the properties of a vortex: it retains "its" particles and does not allow external particles to enter it (see Sec. 3.2.3 below). In addition, after "its" precipitation pours out, stagnation phenomena such as a prolonged drought can be observed in the region of the Rossby vortex [for example, such as occurred in our country (USSR) in 1972]. These are the so-called blockings.[18] If the wind velocity exceeds the value indicated above, the Rossby wave is carried along by the (oppositely directed) wind eastward. It is interesting to note that the propagation velocity of very long Rossby waves ($\lambda \gg r_R$, $k^2 r_R^2 \to 0$) is unaffected by wind: the displacement of the wave by the wind is precisely compensated by the increase in the velocity of the wave relative to the wind owing to the effect of the hydrostatic pressure gradient that appears. For this reason a Rossby soliton[5] is not displaced by the wind (flow).[44]

1.5. Analogy with drift waves in a plasma

There is a profound analogy between Rossby waves and the so-called drift (gradient) waves in plasmas, confined transversely by a strong longitudinal magnetic field. In the case of drift waves the Lorentz force plays a role analogous to that of the Coriolis force. The drift waves appear as a result of the transverse (relative to the magnetic field) nonuniformity of the electron temperature or plasma density, just like Rossby waves appear owing to the transverse (relative to the local angular velocity of the system) nonuniformity of the Coriolis parameter or depth of the liquid. The spatial scale of the dispersion of drift waves is the "Larmor radius of the ions at the electron temperature," analogous to the Rossby-Obukhov radius r_R and equal to the ratio of the ionic sound velocity c_s to the Larmor rotational frequency of the ions in a magnetic field (ω_{rot}), while the quantity ω_B is analogous to the Coriolis parameter f_0. The quantity $kT_e/M = c_s^2$ is analogous to the specific hydrostatic pressure g^*H. The analog of the Rossby velocity is the characteristic drift velocity v_{dr}, whose magnitude and sign are determined by the spatial (transverse) gradients of the plasma parameters and of the magnetic field; this velocity is proportional to the "drift" coefficient β_{dr}, analogous to the coefficient β for Rossby waves (11). The spatial orientation of drift waves is determined by the wave numbers k_x and k_y, corresponding to the azimuthal coordinate x (along the "parallel" around the direction of the magnetic field) and the radial

coordinate y (across the magnetic field). Based on what we just said, it is understandable that the dispersion equation for drift waves is analogous to the equation for Rossby waves. The indicated analogy between the two types of waves in such different media, according to the recollections of M. Obukhov, was first pointed out by M. A. Leontovich about 20 years ago, and was then studied by other authors (see, for example, Refs. 45 and 46). It follows from this analogy that analogously to hydrodynamic Rossby drift solitons, observed experimentally (Sec. 3), drift solitons should also exist in a magnetized plasma.

2. ROSSBY SOLITONS (BRIEF OUTLINE OF THEORETICAL RESULTS)

2.1. Solitary Rossby wave as the result of equilibrium between dispersion and nonlinearity

The following association of dispersion and nonlinearity [see relation (7)] is characteristic of Rossby waves: dispersion is negative (the phase velocity decreases with increasing wave number), while the nonlinearity is positive [the phase velocity (7) increases as the wave amplitude, i.e., the height of the liquid H increases (since $r_R^2 \sim H$)]. This association of properties is a necessary prerequisite for the existence of a solitary wave— (rotating) hump in a liquid with a free surface (Fig. 1). In reality, the sides of the hump (steep slopes of the profile)[6] correspond on one side to the lowest phase velocity (owing to the negative dispersion) and on the other to the highest phase velocity owing to the positive nonlinearity; as a result, it is possible (it has not been excluded) that the dispersion spreading of the wave packet (which is characteristic of a classical linear wave packet) can be compensated by nonlinear self-compression of the packet resulting in the formation of a solitary wave (soliton). It is easy to see that in the case of a negative-elevation wave (a profile with a depression) the effects of dispersion and nonlinearity would be oriented in the same direction, and the nonlinearity would only intensify the dispersion spreading. The theory therefore predicts that a solitary negative-elevation wave is impossible in this case.[7] But the equilibrium hump studied here (radius a, amplitude ΔH), according to the equation of geostrophic equilibrium (2),

$$f_0 v \approx \frac{g^* \Delta H}{a}, \qquad (2')$$

must rotate in a direction opposite to the local rotational velocity of the system: in this case the Coriolis force, acting on the circular current of particles in the vortex, is oriented toward the center of the vortex and balances the hydrostatic pressure associated with the hump. Therefore, the expected Rossby soliton can be an anticyclone but not a cyclone. In a medium with uniform H the soliton must propagate westward.

The qualitative considerations presented above also enable us to estimate the possible size of the soliton. Indeed, from the dispersion equation (6) and the graph in Fig. 2 it is evident that for Rossby waves with a long wavelength ($k^2 r_R^2 \ll 1$) there is no dispersion and nonlinearity predominates; for short waves, on the other hand, dispersion predominates; conventionally speaking, the long waves separate from the short waves near the point $k \approx 1/r_R$, corresponding to the maximum of the dispersion function $\omega(k)$. For this reason, mutual compensation of dispersion spreading and nonlinear self-compression (which must result in the formation of a soliton) is possible only at locations where both the nonlinearity and dispersion are significant, i.e., somewhat to the left of the extremum point, $k_x \approx 1/r_R$. This means that the characteristic size of the soliton must be somewhat greater than r_R. In addition, the higher the amplitude, the farther to the right the soliton is located in Fig. 2, i.e., the smaller the soliton is.

The above considerations illustrate the physical significance not only of the "scalar" but also of the "vector" monopolar Rossby soliton. This follows from the fact[49] that the vector soliton (one of whose dimensions is much larger than the other, and is greater than the radius r_R—like in the JGRS) is also described by an equation of the KdV type, whose soliton solution, as already pointed out, physically corresponds well to the qualitative analysis presented here.

2.2. Monopolar (solitary) Rossby solitons. Theoretical soliton model of the Jovian Great Red Spot (JGRS)

Soliton solutions for solitary Rossby waves have been found in theoretical studies of Refs. 39b, 41, 42a, 47–58 in particular in application to the problem of the JGRS. These studies were preceded by the papers of Ref. 50. In Ref. 50a the vortex of the JGRS was interpreted on the basis of a "Taylor column"—a beautiful hydrodynamic phenomenon,[4b] whose physical meaning follows directly from Oertel's

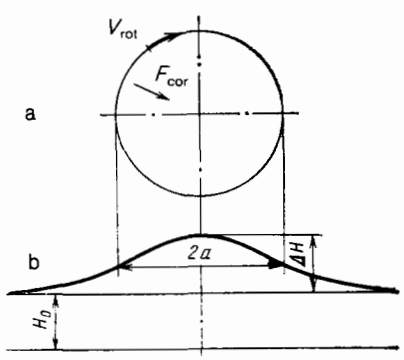

FIG. 1. Anticyclone—equilibrium rise in the surface of a rotating incompressible liquid. F_{cor} is the Coriolis force. a) Trajectory of a particle in the vortex, b) height profile of the liquid.

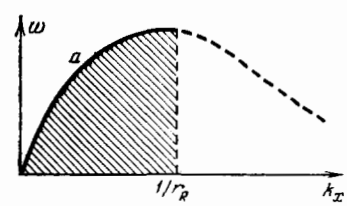

FIG. 2. Dispersion curve for Rossby waves: dependence of the angular frequency of the wave on the wave number k_x, corresponding to the motion along the parallel.

theorem about the conservation of a potential vortex[23–25] (see Sec. 1.3). Consider a flow in rotating shallow water over a solid underlying surface, containing a topographic feature—a "stump" (i.e., a location over which the thickness of the layer of liquid H is less than at neighboring locations). Then the indicated theorem

$$\frac{d}{dt}\left(\frac{\text{rot}\,\mathbf{v}+\mathbf{f}}{H}\right)_z = 0 \qquad (18)$$

implies that above the stump the total vorticity of the flow [the number in the numerator in (18)] will be less than in neighboring locations, i.e., an anticyclonic vortex will exist above the stump (in addition the first and second terms in the numerator have different signs). According to Ref. 50a, the anticyclonic vortex of the JGRS is associated precisely with such a topographic feature. It is now known, however, that, first of all, there is no solid surface beneath the clouds of Jupiter (the gaseous atmosphere extends to the deepest layers of the planet, and there is "no place to drive in a stump," and, second, the vortex of the JGRS drifts relative to the planet (circling the planet along the entire parallel over a period of 10–15 years). Therefore the hypothesis of Ref. 50a is now of only historical interest. In Ref. 50b, under a number of simplifying model assumptions, it is shown by a numerical method that the well-known equation for a vortex in a system with oppositely directed zonal atmospheric flows (see below) implies that a vortex whose characteristic size is much greater than the Rossby-Obukhov radius can exist even if there is no underlying surface (as in the case of the JGRS).

Among the soliton models of the JGRS we call attention first to the chronologically earliest (within the last ten years) theoretical model.[49] Its main results are as follows. 1) A Rossby soliton exists in Jupiter's atmosphere against the background formed by oppositely moving zonal flows, whose velocity in the west-east direction varies along the meridian both in magnitude and in sign (Fig. 3).[8)] 2) The Rossby soliton is a solitary (monopolar) vortex, whose dimension along the parallel is much larger than the dimension along the meridian. 3) The Rossby soliton can be either barotropic (two-dimensional) or baroclinic (three-dimensional) and is characterized correspondingly either by an external or internal Rossby radius (Sec. 1.4). 4) The main type of nonlinearity responsible for the formation of the Rossby soliton is the vector nonlinearity. 5) The solution obtained in Ref. 49 has the form of a soliton and corresponds qualitatively to the observed properties of the vortex of the JGRS: like in the observations, the Rossby soliton is a westward drifting anticyclone whose size exceeds r_R. This model has certain difficulties. One difficulty is that it predicts a much too high drift velocity of the vortex, exceeding the observed value by approximately an order of magnitude. This result is obviously linked with the fact that the scalar nonlinearity was ignored (see Ref. 42).

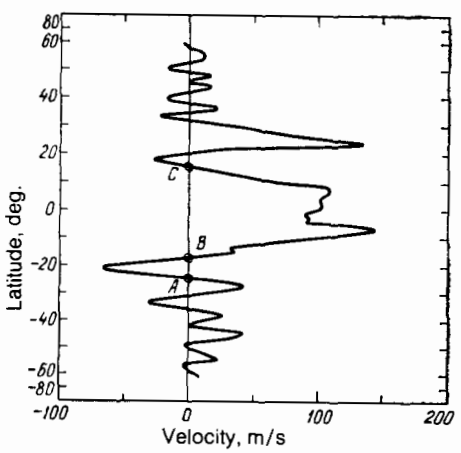

FIG. 3. Zonal flows in the Jovian atmosphere: wind velocity (m/s) as a function of the geographic latitude.[37,61]

With regard to the problem of the JGRS, one must, of course, first consider those papers in which the soliton solutions for Rossby waves (vortices) are obtained in the form of structures which are *self-consistent* with the oppositely moving zonal flows existing in planetary atmospheres: these flows drastically affect the nature of the nonlinearity of the wave studied as well as the possibility of the formation of steady-state solitary vortex structures. In this connection, following Ref. 49, we call attention to the theoretical articles of Refs. 56–58, where model situations, in which either the vector[56,58] or scalar[57a] nonlinearity of the Rossby waves predominates, are studied.[9)] In Ref. 42 both of these nonlinearities are taken into account at the same time in a detailed numerical study, in particular, in application to the JGRS. The results of Ref. 42 also demonstrate the asymmetry studied in Secs. 1.3 and 2.1 in the possibility of the existence of solitary vortices with different polarity: the anticyclones are the only nondecaying structures.

In another group of theoretical studies,[41,54,55,70,73,98] solutions of the monopolar Rossby soliton type were found under conditions when there are no zonal flows, i.e., when the shallow water rotates as a whole (of course, in the presence of the β effect, described in Sec. 1.2). Thus a particular solution for a Rossby soliton, linked predominantly with the scalar nonlinearity, previously known in oceanography,[43,10)] was found in Refs. 41, 54, 55. In the first of these studies,[54] such a soliton was studied in application to vortices in the ocean and for this reason was assumed to be *quasi*-two-dimensional (baroclinic; see Sec. 1.4). In the second variant,[41,55] the Rossby soliton is two-dimensional (barotropic). The physical meaning of the soliton is, of course, the same in both variants. According to Refs. 41, 54, and 55 the Rossby soliton is an anticyclonic vortex with an oval (nearly circular) shape, rotating in the state (3). Its profile is determined by a function of the hyperbolic secant type. In the barotropic case[41,55] its characteristic size (radius) is much larger than the Rossby-Obukhov radius (8); there is a definite relation between the radius (a) and the amplitude (the relative rise in the liquid $h = \Delta H/H$): the diameter of the vortex is

$$2a \approx 3.5\, r_R h^{-1/2}, \qquad (19)$$

and in addition it is assumed that $h \ll 1$. The soliton propagates westward with a velocity somewhat higher than the Rossby velocity (11, 12):

$$V_{dr} > V_R. \qquad (20)$$

In the baroclinic variant[54] the parameters of the soliton are analogous to those just discussed, but the internal radius of the deformation (16), rather than the external radius of the deformation r_R (8), plays the role of the characteristic size of the dispersion.

A substantially different variant of a two-dimensional anticyclonic monopolar Rossby soliton of size $a > r_R$ is studied in the theoretical papers of Refs. 73 and 98, where a qualitatively new effect is taken into account: the trapping of particles of liquid at the center of the soliton.[11)] Such a region appears in the soliton at some amplitude h of the soliton, so that in Refs. 73 and 98, unlike Ref. 55, h is not assumed to be small and can reach 1. The trapped particles, rotating around the axis of the vortex with velocities V_{rot}, exceeding the drift velocity of the vortex (20) [see the relation (40) below], give the soliton new properties. Amongst them we should note first of all the existence, in the trapping region, of "memory" of the initial disturbance (which was responsible for the formation of the soliton), or, in other words, the nonexistence—unlike (19)—of a definite relation between the amplitude of the soliton and its characteristic size. It is fundamentally important that such solitons, which have quite arbitrary (in the indicated sense) sizes and amplitudes, are attractors. This means, in particular, that they are independent of the particular solution (19).[55] In addition, since there are many Rossby vortex solitons of the type under study, while the solution of (19) is unique,[55] it follows that the probability for the realization of the solution (19)[55]—for a sufficiently large amplitude of the vortex (when it carries trapped particles)—is practically vanishingly small. It is important to keep this circumstance in mind both when comparing theory with the experimental data examined below (Sec. 3.3) and in discussions of the soliton model of the JGRS (Sec. 5.1).

Thus comparison of these two variants of the theory of the "scalar" Rossby monopolar soliton leads to the following conclusion: the set of vortex Rossby solitons exhibiting "memory" in the region of trapping of the particles[73,98] contains a soliton which is characterized by a fully determined shape and a relationship between the width and amplitude of the type (19); it is described by an analytic solution,[41,55] distinguished by the continuity of the derivatives of the vorticity; against the overall background formed by these "equivalent" vortex solitons the indicated solution obviously has a very small specific "statistical weight" and, apparently, a correspondingly low probability of realization (ignoring some special method for generating it).

Returning to planetary vortices in the atmospheres of Jupiter and Saturn, we note that not only the JGRS but also virtually all large long-lived vortices on large planets are apparently Rossby vortices. The fact that (see Sec. 5) almost all vortices of large planets, similar to the JGRS vortex, are anticyclones, i.e., they exhibit a cyclone-anticyclone asymmetry, is intriguing. The "lenses" mentioned above—baroclinic vortices on the branch of internal Rossby waves in oceans (see Sec. 5.4)—are also anticyclones.

In concluding this section, we note the following interesting effect. The Rossby soliton is not carried away by a zonal flow (i.e., it is not blown away by a zonal wind). This is demonstrated by simple calculations,[4] whence it follows that the Coriolis force deflecting the zonal flow gives rise to a compensating pressure gradient (oriented along the meridian) in whose field the Rossby velocity (11) and (12) changes precisely by an amount that compensates exactly the displacement of the vortex by the flow. (The linear Rossby wave is subjected to this effect only in the asymptotic case $\lambda \to \infty$; see Sec. 1.4.)

2.3. Dipolar Rossby solitons

The possibility of existence of a dipolar Rossby vortex, which has the form of a symmetric pair of cyclone-anticyclone vortices, propagating in a medium at rest, was predicted theoretically in Ref. 51. This vortex is formed by the vector nonlinearity under the condition (15b). In the interior region of the vortex, bounded by some separatrix, the streamlines are closed—this is the region where particles are trapped by the vortex; in the outer region, the streamlines are open. The anticyclone corresponds to a rise and the cyclone corresponds to a depression (the average level of the liquid in the soliton remains unchanged). The vortex differs fundamentally from the one that is described in the books by Lamb and Batchelor[71,72] by its solitary nature, which is a result of the combined effect of the nonlinearity and the β effect: at a large distance from the center of the vortex the rotational velocity decreases exponentially as a function of the distance, unlike Refs. 71 and 72, where the velocity profile corresponds to the r^{-2} law. In addition, the characteristic length (analogous to the Debye radius in a plasma) is $a = (u/\beta)^{1/2}$ where u is the velocity of the soliton and β is a parameter determining the Rossby velocity according to (11), (12). For example, if $u = v_R$, then $a = r_R$.

The soliton under consideration has the following feature: in a medium with a free surface and a constant depth the velocity of the soliton can lie only in the following ranges:

a) $u > 0$,

b) $u < -V_R$; (21)

in the first case, by definition, it moves eastward and in the second case it moves westward with a velocity greater than the maximum velocity of Rossby waves. The physical meaning of the conditions (21) is that the velocity of the vortex lies outside the range of velocities of Rossby waves [see (7, 12)], and therefore the vortex does not lose energy to Cherenkov emission of these waves; in other words, the relations (21) express the condition for the dipolar vortex to be a steady-state one.[12)] The theory also predicts the existence of a paired soliton such that the partners are not symmetric; it is called a "rider," while a more general name for the paired vortex is "modon."[51] Experiments with such vortices are described in Sec. 8.

2.4. Questions regarding structural stability and steady-state behavior

The question of the stability of Rossby solitons has thus far been studied only within the traditional "β-plane ap-

proximation," in which it is assumed that the Rossby velocity is constant, i.e., it is not a function of the coordinates. In this approximation, according to Ref. 74, the monopolar solitons studied above are stable. On the other hand, if the fact that a real system (for example, a planet), in contrast to the osculating β plane, has a finite curvature (which is, strictly speaking, the origin of Rossby waves) is taken into account and it is assumed that $V_R = r_R^2 \beta(y) \neq \text{const}$,[13] then, also according to the theory of Refs. 42, 57, and 70, the monopolar soliton is subject to additional "nonviscous damping," which causes the vortex to decay into a zonal flow; the decrement of this decay is

$$\gamma_R \approx \frac{1}{2} \frac{\partial V_R}{\partial y} . \quad (22)$$

The physical meaning of this phenomenon is that the points of the vortex with different meridional coordinates (y) drift with different velocities, and the vortex gradually decays. Clearly one can talk about solitons in this case only if the time $1/\gamma_R$ is much longer than the characteristic dispersion time (see Sec. 3.1.2). This condition, as will be shown in Sec. 3.1.3, imposes quite strict requirements on the parameters of the experimental apparatus for generating and identifying Rossby solitons.

The stability of dipolar Rossby solitons has not yet been studied analytically.

The question of the reality of soliton structures can hardly be resolved with definiteness theoretically—further input from experiments is apparently necessary.

3. ROSSBY SOLITONS IN ROTATING SHALLOW WATER (EXPERIMENT)

3.1. Experimental observation of a Rossby soliton and its properties

3.1.1. Brief history of the question

The possibility in principle of observing a "scalar" Rossby soliton in a layer of shallow liquid, rotating together with a parabolically shaped vessel, was pointed out in Ref. 55. This stimulated the beginning of the first stage of experiments on the observation of Rossby solitons in which the *liquid rotated as a whole* together with an approximately parabolically shaped vessel.[78–82] These experiments were undertaken only after experimenters[96] developed physical criteria which parabolic models must satisfy so that vortices like the Rossby solitons could be unequivocally identified in them. These criteria are presented in Sec. 3.1.3. A Rossby soliton was first created in the laboratory in the experiments of Refs. 78–82, which satisfied these criteria. It was shown that a Rossby soliton exists in the free state (without replenishment) for approximately the viscous time period (about 20 sec). These experiments qualitatively agreed with the then-existing theory[55] (and also Refs. 41 and 54), they revealed the obvious clear disagreements with the theory, and, most importantly, they revealed a number of new fundamental properties of Rossby solitons, which were not contained in the existing theory (see Sec. 3.2). This broadened the concept of Rossby solitons and stimulated the development of the theory (it also led to the development of a new theory,[73,98] the main results of which are presented in Sec. 2.2).

This completed the first stage of experiments, associated with the study of monopolar Rossby solitons in a liquid rotating as a whole (dipolar vortices were studied somewhat later[96]). After this, the second stage of the experiments began—the study of coherent vortex structures in a new geometry of the system, namely, with a *differentially rotating liquid*, in which oppositely moving flows, physically similar to zonal flows in planetary atmospheres, were superposed on the basic rotation of the system as a whole. This stage of experiments was no longer linked with the theory.[5] At this second stage (see Refs. 82–86) two instabilities of shear flows were discovered: the Kelvin-Helmholtz (KH) instability and the centrifugal instability (CI), which lead to the generation of chains of large-scale vortices (whose size exceeds the Rossby-Obukhov radius), arranged along the perimeter of the system; under certain conditions these vortices are Rossby solitons. Next, at the third stage of experiments,[87,88] performed on a modified experimental arrangement with a new geometry, a regime of zonal flows in which their instability leads to the formation of a new nonlinear vortex structure—*a Rossby autosoliton*—was discovered. The latter is a solitary nondecaying large-scale ($a > r_R$) anticyclonic vortex, which is *the only one* over the entire perimeter of the system, self-organizing in flows, and representing a steady-state physical soliton model of natural vortices of the JGRS type. [We note here that this is an instructive example of how the instability leads not to small-scale turbulence, but rather to the formation of large coherent structures (see also Refs. 11, 75–77, 90, 91, 96, 97).] The indicated experiments made it possible to explain simply the fact that all large vortices on Jupiter and Saturn are anticyclones, with the single exception of the Brown Ovals ("barges") on Jupiter (14 °N.L.), as well as the physical meaning of this exception.[4] (We note that the large-scale *cyclonic* vortices, existing on Jupiter as an exception, could be of the same nature and could be generated by the same mechanism as cyclones which under terrestrial conditions are nonexceptional; see Sec. 5.)

Experiments (also with differentially rotating shallow water) on modeling the hydrodynamic mechanism of the generation of the spiral structure of galaxies which have a jump in the velocity on the rotation profile were conducted in parallel with the experiments on the generation of Rossby solitons by flows.[89–90]

These experiments suggested that both natural phenomena—large vortices in the atmospheres of large planets and the spiral structure of galaxies of the type indicated above—are apparently generated by the same physical mechanism. They are based on the hydrodynamic instability of differentially rotating "shallow water" (the core rotating more rapidly than the periphery[91]). The theory of this instability is discussed in Refs. 92–94.

Before describing the experiments we shall clarify the formulation of the problem.

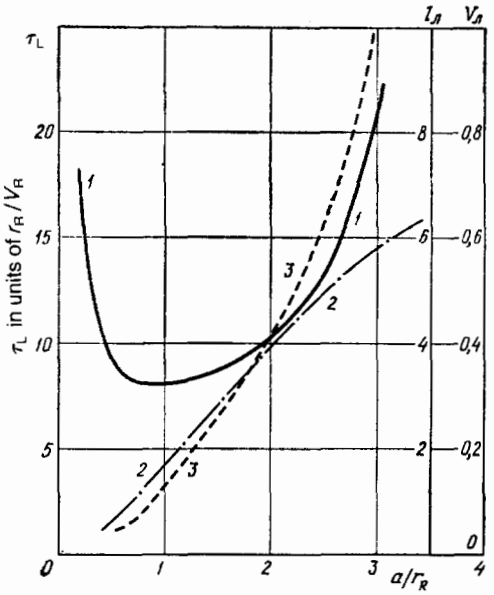

FIG. 4. The effective time τ_L (curve 1) of dispersion spreading of a linear packet of Rossby waves (in units of r_R/V_R) as a function of the diameter of the packet (in units of r_R). Starting formula of the packet: $h = h_0 \exp(-r^2/a^2)$. The time τ_L is defined as the time over which the amplitude of the wave packet decreases by a factor of 2.[95] The figure also shows the change in the drift velocity (curve 2) and the range of the packet (curve 3).

3.1.2. Formulation of the problem. When is a vortex a soliton? The lifetime and range of a linear two-dimensional packet of Rossby waves

In order to identify unequivocally in experiments a Rossby vortex as a soliton it is necessary to show that it exists without decaying for a period of time (τ) which greatly exceeds the time (τ_L) of dispersion spreading of a linear two-dimensional packet of Rossby waves of the same size:

$$\tau > \tau_L. \tag{23}$$

The problem of dispersion spreading of a linear two-dimensional (circular) packet of Rossby waves in the β plane was solved theoretically in Ref. 95. The result is presented in Fig. 4, which shows three of its parameters as a function of the diameter of the packet (which initially is Gaussian): the characteristic lifetime (τ_L), the westward propagation velocity (V_L), and the range over the lifetime (l_L). The quantity τ_L corresponds to a decrease in the amplitude of the packet by a factor of two and is expressed in units of r_R/V_R, the diameter of the packet (the distance between antipodal points on the profile at which the rotational velocity of the particles equals $1/e$ of the maximum value) and l_L are expressed in units of r_R, while v_L is expressed in units of V_R. There is a minimum spreading time: it corresponds to the diameter of the packet $2a \approx 2r_R$ and constitutes

$$(\tau_L)_{\min} \approx \frac{8r_R}{V_R}. \tag{24}$$

The propagation velocity V_L of a linear Rossby packet of the dimensions under study, is significantly lower than the Rossby velocity. Thus, for a packet of size $2a \approx (2\text{–}3)r_R$, $V_L \approx 0.2V_R$. Such a packet can traverse over the dispersion spreading time (24) a distance

$$l_L = V_L \tau_L \lesssim 2r_R \approx 2a; \tag{25}$$

thus the "free path length" of a linear two-dimensional packet of Rossby waves with a minimum dispersion spreading time equals approximately one diameter of the packet. In addition, since the Rossby soliton must move with a velocity greater than V_R, i.e., several times faster than a linear packet, and its lifetime must be longer, the path l_s traversed by the soliton over its lifetime must also be much greater than its diameter $2a$:

$$l_s \gg 2a. \tag{26}$$

If a soliton whose radius is greater than r_R carries captured particles, i.e., it is a "real" vortex (for which $V_{rot} > V_R$), then it satisfies the condition

$$N \gg 1, \tag{27}$$

where N is the number of times the vortex can revolve around its axis over its lifetime. This condition is equivalent to (26).

3.1.3. Experimental arrangement—parabolic model of the atmosphere (ocean) of planets. Requirements on the model paraboloid

The free surface of a liquid rotating in the gravitational field with a constant angular velocity Ω about a vertical axis (Fig. 5) assumes a parabolic shape according to the equation

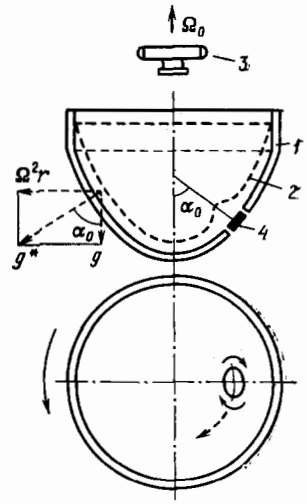

FIG. 5. Equilibrium layer of liquid in a rotating paraboloid and the layout of the experimental arrangements[78–82,96] used for exciting and studying solitary (monopolar) and dipolar Rossby solitons in shallow water rotating as a whole. 1) Vessel with approximately parabolic bottom profile; 2) water surface spreading under rotation along the parabolic bottom; 3) camera (or motion picture camera), rotating together with the vessel; 4) rotating pumping disk. The paraboloid rotates counterclockwise around the vertical axis with an angular velocity Ω. View from above: the solid arrows indicate the anticyclonic direction of rotation of the pumping disk and the direction of rotation of the vessel; the broken arrow shows the direction of drift of the Rossby soliton in the absence of a gradient of the depth of the liquid (the soliton lags behind the global rotation of the system). The angle α is the angle between the rotational axis of the vessel and the normal to the surface of the liquid at the working point.

$$z = \frac{\Omega^2 r^2}{2g} = pr^2, \tag{28}$$

which follows immediately from the condition of equilibrium of the forces acting in the plane tangent to the surface of the liquid: $\Omega^2 r \cos\alpha = g \sin\alpha$, whence $\operatorname{tg}\alpha \equiv dz/dr = \Omega^2 r/g$, where z and r are the distances of a point on the surface from its lowest point, measured along the rotational axis and in a perpendicular direction, respectively; g is the acceleration of gravity. The parameter

$$p = \frac{\Omega^2}{2g} \tag{29}$$

characterizes the steepness of the paraboloid.

The layer of rotating liquid can be used as a model of the uniform atmosphere (ocean) of a planet, if its thickness is constant, i.e., if the bottom of the vessel rotating together with the liquid has an approximately parabolic shape, close to (28). More precisely, the following stipulation must be made: if the bottom and surface of the liquid have the same shape, then the thickness of the layer of liquid will be constant not along the normal to the surface, but rather along the z axis; therefore in order for the thickness of the layer H_0 to be constant in a direction toward the normal to the surface of the liquid, the vessel must be somewhat more gently sloping than (28). It is precisely vessels of this type that were used in all of the described experiments[14]; we shall refer to them briefly as paraboloids (see Fig. 5). In a rotating paraboloid the layer of liquid is subjected to the resultant of two forces: the force of gravity and the centrifugal force from the global rotation of the system as a whole; under the conditions of equilibrium the acceleration of the resultant is oriented along the local normal to the surface of the liquid and is given by (Fig. 5)

$$g^* = \frac{g}{\cos\alpha}. \tag{30}$$

Using the formula (30), in a paraboloid with $H = \text{const} = H_0$ we have

$$r_R = \frac{(gH_0)^{1/2}}{2\Omega_0 \cos^{3/2}\alpha}, \tag{31}$$

$$V_R = g^* \frac{\partial}{\partial y}\frac{H}{f} = \frac{g^*}{R}\frac{\partial}{\partial\alpha}\frac{H}{f} = \frac{1}{2} H_0 \Omega_0 \sin\alpha, \tag{32}$$

where R is the radius of the meridional curvature of the paraboloid:

$$R = \left[1 + \left(\frac{\partial z}{\partial r}\right)^2\right]^{3/2} \left(\frac{\partial^2 z}{\partial r^2}\right)^{-1}.$$

and, according to (4), $f = 2\Omega_0 \cos\alpha$.

We shall indicate here one more result, which is important for experiments. If the angular rotational velocity of the paraboloid Ω exceeds the value Ω_0 at which $H = \text{const}$ by an amount $\Delta\Omega$, then the depth of the liquid will have a meridional gradient directed toward the periphery of the vessel (and when $\Delta\Omega$ has the opposite sign the gradient is directed toward the center of the vessel). In addition, the Rossby velocity (11) according to (32) will be different, since $H \neq \text{const}$. The simplest expression for V_R is obtained for the parallel on the paraboloid which is located at a distance $r_0 = R_0/\sqrt{2}$ from the rotational axis, where R_0 is the radius of the vertical cylinder bounding the transverse dimension of the paraboloid. On this parallel, for small $\Delta\Omega/\Omega$, the thickness of the layer of liquid is constant, and according to Refs. 79 and 78[15]

$$V_R = \frac{1}{2} H_0 \Omega_0 \sin\alpha \left[1 + \frac{\Delta\Omega}{\Omega_0} \frac{2R/H_0}{1 + (\Omega_0^2 R_0^2/2g^2)}\right]. \tag{33}$$

It is evident that when $\Delta\Omega > 0$ the quantity V_R increases (the vortex drifts westward even more rapidly than for $\Delta\Omega = 0$; for $\Delta\Omega < 0$ the Rossby velocity decreases and can even change sign [then the vortex will drift eastward, as does happen (see Sec. 3.1.4 and Fig. 7b)].

We shall now formulate the criteria which the parameters of the paraboloid with shallow water must satisfy in order for the vortices observed on it to be identified as Rossby solitons (in other words, in order that the paraboloid be suitable for observation of Rossby solitons).[96] The first criterion follows immediately from (23), (24), and (8):

$$p \sin 2\alpha > \frac{8}{\tau (gH_0)^{1/2}}, \tag{34}$$

where $p = \Omega_0^2/2g$ is the steepness parameter of the paraboloid. The quantity τ is bounded from above by the viscous time, τ_{vis}. In reality, in the experiment studied below, τ_{vis} does not exceed several tens of seconds. Therefore it follows from (34) that the paraboloid must be quite steep and that the working region must be located quite far away from its pole. [The condition (27) leads to the same result.] For later comparison of the criterion under study with the conditions of the experiments described below, we shall take two examples:

1) Let $H_0 = 0.5$ cm, $\sin 2\alpha \approx 1$, $\tau \approx 20$ s. Then (34) gives

$$p > 2 \cdot 10^{-2}\ \text{cm}^{-1}. \tag{35a}$$

2) Let $H_0 = 2$ cm, $\sin 2\alpha \approx 1$, $\tau \approx 20$ s. Then (34) gives

$$p > 10^{-2}\ \text{cm}^{-1}. \tag{35b}$$

The second criterion is associated with the "β-plane approximation," introduced by Rossby[7] and widely used in the theory of Rossby waves and solitons (see Refs. 24, 23, 51, 74, 70).[16] According to this approximation in the tangent plane to the paraboloid in the working region, $V_R \approx \text{const}$, i.e., the change in V_R over the meridional size of the vortex (L) is small compared with V_R:

$$\frac{L}{R}\frac{\partial V_R}{\partial\alpha} \ll V_R,$$

which combined with (32) means

$$\operatorname{tg}\alpha \gg \frac{L}{R}. \tag{36}$$

This criterion also implies that the steepness of the paraboloid must be quite large and the working region must be located quite far away from the pole of the paraboloid.

We obtain an analogous estimate from the requirements (23), (24), according to which the lifetime of the vortex τ, which is limited by the variability of the Rossby velocity over the size of the vortex, $\tau \approx 2(\partial V_R/\partial y)^{-1}$ [see (22)], must exceed the dispersion time τ_L, defined by (24) as

$$\frac{1}{2}\frac{\partial V_R}{\partial y} < \frac{1}{8}\frac{V_R}{r_R}, \quad (37)$$

or

$$\operatorname{tg}\alpha > \frac{4r_R}{R}. \quad (38)$$

We emphasize the fundamental nature of the requirements (23), (24), and (38). The point is that if these requirements are not satisfied, then the wave packet has time to decay over a time shorter than the characteristic time[95] of the dispersion spreading of a linear packet of Rossby waves. But in this case one cannot say that the wave packet is "nonspreading" (compared with the linear packet of Rossby waves). This means that in this case the wave packet (vortex) cannot be identified as a Rossby soliton (see also Sec. 8.2).

Experiments on the observation and study of Rossby solitons in a thin layer of liquid rotating as a whole[78–82] were carried out on two paraboloids—"small" and "large," which are shown in Fig. 5 and whose parameters are presented in Table I. These parameters were carefully chosen—for the working region, *a* in Fig. 2, and starting from the criteria (34)–(38). For this reason the paraboloids were made to be quite steep. It is not difficult to see that for the actually observed lifetime of vortices (about 20 s) the parameters of the experimental arrangements being studied satisfy the indicated criteria. We note that as a special theoretical investigation showed,[129] the effect of capillarity on Rossby waves in these (and, by the way, in all other realistically imaginable) experiments can be completely ignored. A vortex was excited in these experiments by two methods. In one method a "pumping disk," placed on some "latitude" of the paraboloid in the plane of the bottom and switched on for several seconds, was used; the diameter of the disk could be varied from one experiment to another. In the other method, a jet of water was injected in a pulsed manner into the working liquid (water) from a short tube near the bottom of the paraboloid; the action of the Coriolis force on this jet formed a vortex (anticyclone). Both methods gave the same results. In order to photograph the vortices (which was usually done with a camera rotating together with the vessel, and sometimes together with the vortex) the working liquid (water) was colored with a dye, and white test particles were floated on its surface. When the vortices were photographed in red light, passing through a green solution and reflected from the white bottom of the vessel, the rise in the liquid (anticyclone) appeared to be darker than the depression (cyclone). Photometric measurements of the photographs obtained made it possible to determine the profile of the height of the vortex and, in particular, to find the diameter of the vortex. By measuring the length of the tracks of the test particles, traced over the exposure time of the camera, it was easy to determine the entire velocity profile in the vortex. From this profile, with the help of the equation of geostrophic equilibrium (2)

$$2\Omega v\cos\alpha = \frac{g^*\Delta H}{a_m}$$

it was possible to determine independently the amplitude of the vortex $\Delta H = hH_0$, and its size a_m (the corresponding maximum of the linear velocity on the profile).[17] The experimental results obtained with both paraboloids by the indicated independent methods agree satisfactorily with one another. It is important to note that for methodological reasons, associated with the sensitivity of the experimental procedures used, in the experiments described the amplitude of the Rossby vertices was not too low:

$$h \gtrsim 0.15.$$

3.1.4. Observation of a Rossby soliton: its dimensions, profile, amplitude, drift and range

The main results of the experiments performed with the small paraboloid, in which a Rossby soliton was first ob-

TABLE I. Parameters of experimental arrangements.[78–88,96]

Small paraboloid	Large paraboloid
$z = 6\cdot10^{-2}r^2$	$r = 2{,}86\cdot10^{-2}r^2$
$2R_0 = 28$ cm	$2R_0 = 70$ cm
$r_0 = 10$ cm	$r_0 = 25$ cm
$R_y = 32$ cm	$R_y = 90$ cm
$H_{min} = 0{,}3$ cm	$H_{min} = 0{,}5$ cm
$H_{max} = 1{,}2$ cm	$H_{max} = 5$ cm
For $H_0 = 0{,}5$ cm	For $H_0 = 1$ cm
$T_0 = \frac{2\pi}{\Omega_0} = 0.58$ s	$T_0 = \frac{2\pi}{\Omega_0} = 0.84$ s
$r_R = 2{,}1$ cm	For $H = 3$ cm = const $r_R = 7.6$ cm
$V_R = 2{,}2$ cm/s	$V_R \approx 9$ cm/s
$\tau_L \approx 8\frac{r_R}{V_R} \approx 7.6$s	$\tau_L \approx 8\frac{r_R}{V_R} \approx 6.6$ s

$z(r)$ is the equation for the surface of the liquid rotating with a definite frequency (Ω_0); T_0 is the period of rotation of the vessel, corresponding to the layer of liquid with constant depth H_0; $2R_0$ is the maximum diameter of the paraboloid; r_0 is the radius of the working point; R_y is the radius of the meridional curvature of the vessel; τ_L is the minimum dispersion spreading time of a linear packet of Rossby waves.

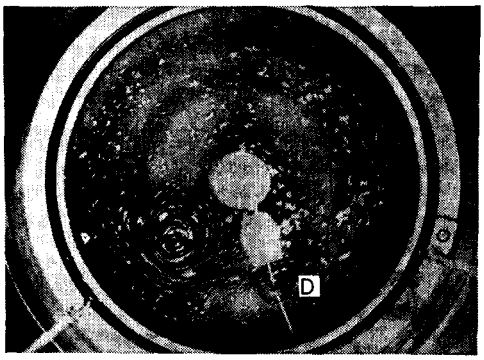

FIG. 6. Example of an anticyclonic Rossby soliton, made visible by white particles floating on the surface of a green liquid, and also by the contrast of the image in red light, passing through the solution and reflected from the white bottom of the vessel.[79] The view from above on the rotating paraboloid is shown. D is the pumping disk, 3 cm in diameter; the white parts are the drive for the disk (above the liquid). The photograph was made with a camera rotating together with the vessel 2 to 3 s after the disk was switched off. The vortex drifts clockwise. $H_0 = 5$ mm.

served (generated), are illustrated in Figs. 6–11 and consist of the following. Figure 6 shows a typical anticyclonic vortex, recorded ~ 3 sec after being generated by the pumping disk D and drifting, for $H = \text{const}$, opposite to the direction of rotation of the vessel.[18)] The profile of its vortex (see Fig. 8) is that of a soliton[79] (approximately Gaussian, dropping off much more steeply than in a classical vortex, where $v \sim 1/r$). The diameter of the vortex (the transverse dimension at the center of the profile) is about 2.5 r_R, the relative amplitude $h \approx 0.5$, and the characteristic frequency of the intrinsic rotation of the vortex (opposite to the direction of the global rotation of the paraboloid) at the center of the dropoff of the profile is about 1/4 of the rotational frequency of the system. According to the parameters indicated, the object under study is a geostrophic vortex in the Rossby state (3), approximately corresponding to the region of maximum dispersion on the curve in Fig. 2 [the region a, to the left of the maximum of $\omega(k)$]. This vortex drifts relative to the vessel, and for $H = \text{const}$ this drift is directed westward, i.e., in the direction of drift of Rossby waves. Figure 7a shows a vortex generated with $H = \text{const}$ by a pumping disk in position 1, colored from above in position 2, drifting clockwise and photographed ~ 20 s after it appeared; the parameters of the vortex are approximately the same as those in the case of Fig. 6. The vortex drifts for 20 s (practically uniformly in time[79]) with a velocity $V_{dr} \approx 2$ cm/s $\approx 0.8 V_R$, where $V_R = (1/2) H_0 \Omega_0 \sin \alpha$ is the Rossby velocity for $H = \text{const}$. This drift velocity is approximately one third of the typical, linear velocity of the vortex rotation which is maximum along its profile (see Fig. 8). The drift velocity of the vortex increases as the depth of the liquid and the amplitude of the vortex increase[82]—in qualitative agreement with Sec. 2.1. The drift velocity of the vortex increases substantially when the rotation of the paraboloid is speeded up and decreases when the rotation is slowed down. At some rotational frequency of the vessel ($\Omega < \Omega_0$) the vortex stops (relative to the vessel), and

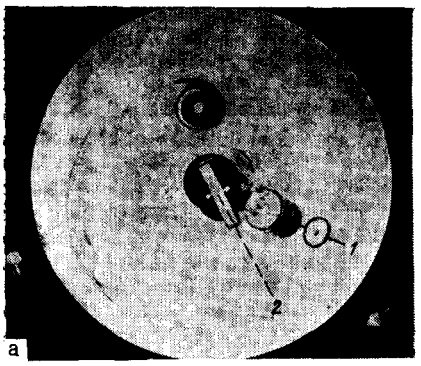

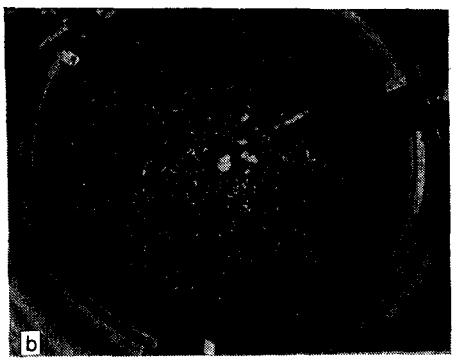

FIG. 7. a) Drift of an anticyclonic vortex opposite to the direction of rotation of the vessel.[79] The vortex is formed in pure water (near the pumping disk 1), it is colored with particles of potassium permanganate (introduced from above with the help of a catapult) in the position 2 and drifts clockwise. The photograph was taken 18 s after the vortex appeared; the lifetime of the vortex equals about 20 s. $H_0 = 5$ mm. b) Drift of Rossby anticyclone in the direction of rotation of the vessel in the presence of a gradient of the depth of the liquid, directed toward the center of the vessel.[96] Large paraboloid. $T = 880$ ms, $H = 1$ cm, the diameter of the pumping disk $D = 10$ cm.

at an even lower frequency it drifts in the opposite direction ("eastward") (see Fig.7b). These facts (in particular, the magnitude of the frequency shift corresponding to stopping

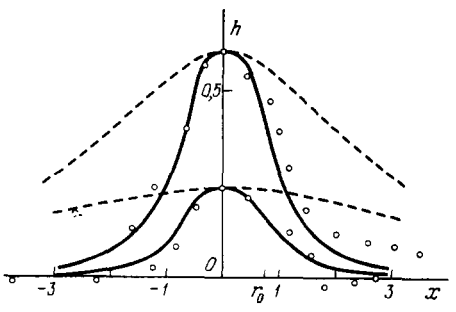

FIG. 8. Comparison of experimental profiles of the rise in the liquid in a Rossby anticyclone (circles) with theoretical profiles.[73] The solid curves correspond to the theory (numerical calculation), demonstrating the existence of a "memory" of the initial conditions in the entire central region of the vortex, where particles of liquid are trapped (the constant potential vorticity is given initially in the region of the central "core" with radius r_0); the broken lines show the particular ("smooth") analytic solution,[73] successfully distinguished from the particular solution[41,45] in practice only by the fact that the restriction $h = \Delta H / H_0 \ll 1$ on the amplitude of the vortex is removed.

of the drifting motion of the vortex), observed on both the small and the large paraboloid, are in good agreement with the relation (33). The dynamics of the Rossby vortex, created by a different method (injection of a jet from a tube), is illustrated in Fig. 9. The characteristic profile of the vortex under study is shown in Fig. 8.

It is interesting to compare the observed lifetime of the vortex under study (τ) and its range l (over which the shape of the vortex remains unchanged) with the analogous characteristics of a linear wave packet. According to (24) for $r_R = 2.1$ cm and $V_R = 2.2$ cm/s, $\tau_L \lesssim 8$ s, while $\tau \gtrsim 20$ s (over a time of 20 s there are no indications of spreading of the vortex (see Fig. 7a). Therefore $\tau \approx 2.5\tau_L$. The velocity of propagation of the vortex studied is also substantially (by a factor of ~ 4) higher than the velocity of a linear packet of Rossby waves with the same dimensions. Correspondingly, as Fig. 7a shows, the observed range of the vortex under study over its lifetime (~ 20 s) equals 10 times the diameter of the vortex, i.e., it is approximately an order of magnitude longer than the range (25) of a linear wave packet. It is in this feature that the soliton nature of the vortex under study is manifested.

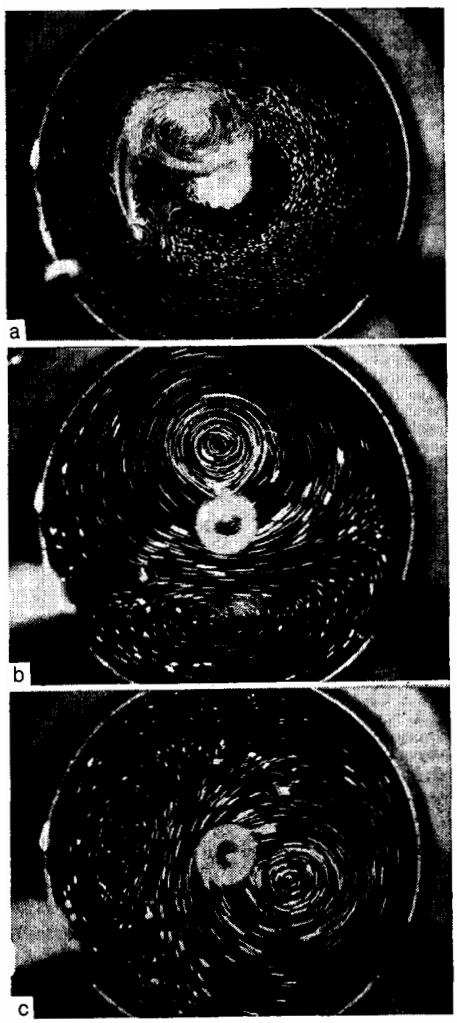

FIG. 9. Drift of the anticyclone created by injecting a jet of liquid. The time intervals between the frames *a–c* equal 10 and 5 s. Small paraboloid (see Table I). In position *b* the vortex made a complete revolution around the vessel.

It is not difficult to see that this vortex also satisfies the condition (27). Indeed, since in these experiments the rotational velocity of the vortex (time-averaged) is several times greater than its drift velocity, the number of revolutions N completed by the vortex around its axis over its lifetime approximately equals the number of characteristic diameters over which the vortex is displaced in the course of its drift motion. From here it follows that in these experiments $N \approx 10$ in accordance with the condition (27). Thus, summarizing the properties of the anticyclonic vortex under study, we arrive at the conclusion that it is a Rossby vortex soliton. The parameters of the soliton, with definite quantitative differences, are close to those suggested by Sec. 2.1.

Experiments with different solutions showed that the above-described dynamics of Rossby vortices is not affected by variations in the viscosity of the medium over an approximately three-fold range; therefore, the viscosity affects only the lifetime of the vortex.

3.1.5. Cyclone-anticyclone asymmetry

All vortices shown in Figs. 6–11 are anticyclones. As regards cyclones, experiments have shown that it is quite difficult to create a Rossby cyclone by rotating the pumping disk in the cyclonic direction. Thus under the conditions of the small paraboloid the following effect is usually obtained: a disturbance of the fluid still generates an anticyclone. A cyclone can sometimes be generated in experiments with the large paraboloid. These experiments (see Sec. 8) show that in successful realizations of the desired vortex its lifetime, drift velocity (it drifts in the same direction as does the anticyclone), and range are practically equal to those of a linear packet of Rossby waves with the same dimensions, namely, for a vortex with the diameter $2a \approx (2 - 2.5)r_R$ the drift velocity is $V_{dr} \approx 0.3V_R$ (much lower than for an anticyclone), $\tau \approx \tau_L$, $l \approx l_L \approx 2a$. A vortex with these characteristics obviously cannot be regarded as a Rossby soliton.

The observed cyclone-anticyclone asymmetry (further sharp manifestations of which are described below) is a very fundamental dispersion-nonlinear property of Rossby vortices. It is a direct consequence of the scalar nonlinearity and corresponds well to the qualitative analysis carried out in Sec. 2.1 and the theory in Refs. 41, 42, 55, 70, and 73. The main effect consists in the fact that in a cyclone, unlike an anticyclone, the nonlinearity and dispersion are not mutually balanced.

So, the facts observed in the experiments examined above are qualitatively predictable based on the existing theory. In the next section we shall examine phenomena which are not described by this theory.

3.2. Experimental "surprises"

3.2.1. Rossby soliton as an attractor

The experiments under study showed[79,80] that an arbitrary (sufficiently extended) initial perturbation of the liquid rapidly evolves into well-formed Rossby vortices (soli-

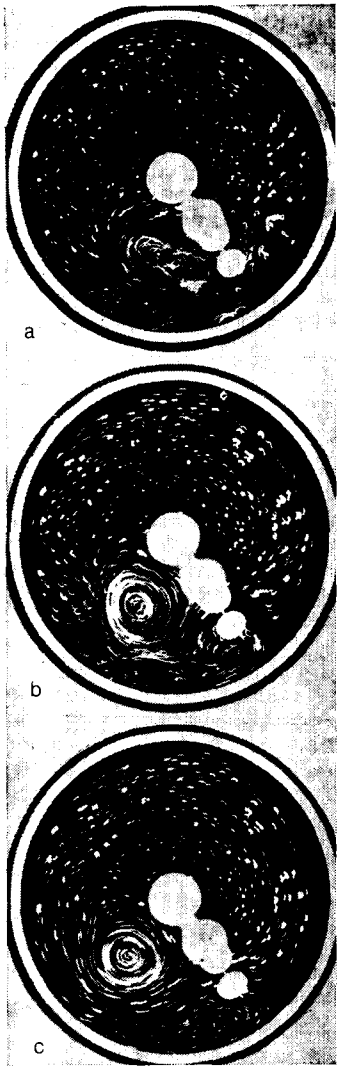

FIG. 10. Formation of an anticyclonic Rossby soliton from an irregular disturbance.[82] $H_0 = 0.3$ cm. The time interval between frames equals 1.2 s (two revolutions of the vessel).

tons). This, in particular, is evident in Fig. 10, which shows the successive positions of the same vortex after definite time intervals. Thus the Rossby soliton is not simply one of the possible particular (amongst many) solutions of the nonlinear equations (the existing theory does not assert any more than this), but rather it is the preferred, or the "attracting," solution. In other words one can say that the (anticyclonic) Rossby soliton manifests the property of an attractor. A Rossby cyclone, as shown above, does not have this property. (Attractors and coherent structures are discussed, for example, in Refs. 76, 77, 11, and 97.)

3.2.2. Stability, lifetime

The experimental data under study definitely shed light on the question of the stability of Rossby solitons, which is not fully studied in the analytic theory. The following facts indicate that these solitons are relatively stable. The first fact is the attractor property of Rossby anticyclones, already demonstrated in the preceding Sec. 3.1. Second, their lifetime is long. As shown above, it is substantially longer than the lifetime of a linear wave packet, and under the conditions of the experiments described it is close to the characteristic viscous decay time

$$\tau \approx \frac{H_0^2}{\nu}, \tag{39}$$

where $\nu \approx 10^{-2}$ cm^2/s. For a typical depth $H_0 = 0.5$ cm, from (39) we obtain $\tau \lesssim 25$ s, which is in good agreement with the experimental data (see, for example, Figs. 7 and 8). Third, as shown by experiments with Rossby vortices of different sizes, excited by pumping disks with different diameters, it is particularly the vortices with the parameters considered here that have the longest lifetimes.[80] Smaller vortices ($2a < 2r_R$) decay relatively rapidly. Vortices which are too large ($2a > 5r_R$) also decay rapidly, but here the required condition that the size of the vortex be smaller than the radius of curvature of the system, is not satisfied. Rossby cyclones under conditions of a shallow liquid can serve as a "standard" for rapidly decaying (dispersing) vortices. Compared with them the anticyclonic Rossby solitons are long-lived stable structures.

3.2.3. Transport of liquid: the vortex property of a Rossby soliton

The properties of the "monopolar" Rossby vortices under study can be predicted well and interpreted on the basis of wave concepts (Sec. 2.1). For this reason, it appeared at first that a monopolar Rossby soliton will propagate in a medium like a wave, without entraining particles of the liquid. Such a concept, in particular, is consistent with Ref. 55, where, as indicated above, it is assumed that $h \ll 1$ and nothing is said about the existence of a region of captured particles in the soliton. However, experiments[19)] (in which, as already indicated, $h \approx 0.5$ cannot be regarded as a small parameter) show that the monopolar Rossby soliton of characteristic size a under study contains a region of trapped particles. Correspondingly, the soliton very effectively transports (without releasing) particles of liquid (contained in it at the moment of generation or injected from above) and does not allow particles which it encounters during its drift motion around the axis of the system to enter it.[79] An example of efficient transport of particles of liquid by a Rossby soliton is shown in Fig. 7a, demonstrating the following experiment. A Rossby soliton is generated in a colorless liquid by a pumping disk in position 1 and drifts clockwise. In position 2 particles of dye are injected into it from above. It is evident that the particles confined in some interior region of the vortex are effectively trapped by it and are transported over large distances, while the outer particles (outside the separatrix) remain outside the vortex. Experiments also show that a region of trapping of the particles inside the Rossby vortex[20)] exists only if

$$V_{\text{rot}} > V_{\text{dr}}, \tag{40}$$

under which condition the particles escaping from the vortex (or flowing into it from outside along the x and y axes) would have to cross the streamlines, and this does not hap-

pen. This condition, as can be easily seen from the equation of geostrophic equilibrium (2′), is obviously satisfied in these experiments under the above-indicated condition $h \gtrsim 0.15$ and it therefore holds in all experiments described above. The fact that a monopolar Rossby soliton contains a region of trapped particles, first discovered experimentally, is now taken into account in the theory (see Sec. 2.2).

3.2.4. Inelastic collisions

The question of the nature of the collisions of solitary waves is fundamental in the theory: there even exists a definition[28,29,51] (although it is not generally accepted and we do not analyze it), according to which a solitary wave is a soliton if its collision with another solitary wave is purely elastic.

The experiments under discussion (to the surprise of the theory,[49,55,97] which ignores the trapping of particles by the soliton) showed that the Rossby solitons under study collide inelastically[81,82]: they either coalesce into one soliton (if they approach one another with a sufficiently high velocity) or they mutually destroy each other, transforming into a flow (when the approach velocity is low). An analogous disagreement between the indicated theory and observations is observed in the Jovian atmosphere.[38] An example of the coalescence of monopolar Rossby solitons, following one another (a large-amplitude vortex, approaching from behind, catches up with the vortex in front of it), is shown in Fig. 11, which shows a series of photographs made at successive times. In connection with the experimental data under study, it should be pointed out that the initial "requirement" of the theory[28,29] that soliton collisions be elastic was associated with the property of one-dimensional solitons, described by the Kortweig–de Vries equation.[29,32] Other solitons exhibit a more complicated behavior. Thus two- and three-dimensional ion-acoustic solitary waves in a plasma, as experiments show,[33] undergo inelastic collisions and they are nevertheless called solitons. The collisional properties of solitons can depend qualitatively on their amplitude. Thus Langmuir solitons whose amplitudes are sufficiently small collide elastically, and if their amplitudes are sufficiently large, they coalesce (with the emission of ion sound).[34]

Here it is important to note that in the theoretical studies of Refs. 42, 98 it is shown (by means of a numerical calculation) that when Rossby vortices, carrying trapped particles, collide they must coalesce—in accordance with the experimental data examined above.

3.2.5. Rossby vortices with $h > 1$

Experiments in which a Rossby vortex was generated by a jet of water, injected in a pulsed manner (over a time interval of ~ 1 s) into a liquid with a shallow depth H_0, gave the following result (see also Fig. 9). If the volume of the liquid injected from the tube is sufficiently large (for example, 100 cm^3), then the height of the hump in the vortex formed, ΔH, is much greater than the starting depth of the liquid H_0 (if the latter is not too large). In addition, formally, $h \equiv \Delta H / H_0 > 1$. Experiments have shown that the lifetime of such "exotic" vortices is approximately the same as

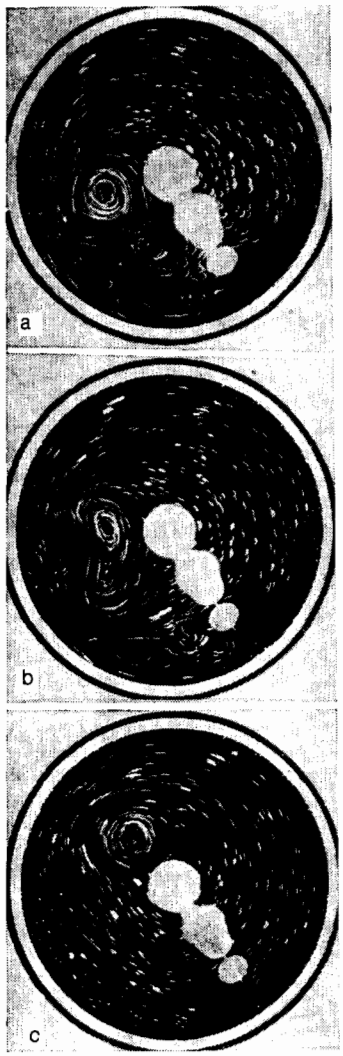

FIG. 11. Different stages of the convergence and coalescence of Rossby anticyclones, created by one pumping disk D.[82] The time intervals between the frames equal 1.2 and 4.2 s.

the lifetime when $h < 1$. In addition, this behavior is observed even for very shallow depths—right up to $H_0 \approx 1$ mm. These facts once again indicate the "roughness" of the soliton structures studied.

3.3. Relationship between theory and experiment

The experimental data presented above show that the theoretical expectations (see Sec. 2.1 and 2.2) are on the whole qualitatively cofirmed by experiments: the Rossby soliton exists in the form of a solitary (monopolar) anticyclone, it drifts in the "correct" direction with approximately the "correct" velocity, and its dimensions $a > r_R$ are close to the predicted values. Thus the examined experiments support the theoretical picture that the scalar nonlinearity plays a fundamentally important role (under the indicated experimental conditions) in the formation of monopolar Rossby solitons with dimensions exceeding the Rossby-Obukhov radius [see (15a)]. A more detailed comparison of experi-

ments with different variants of the theory shows the following. a) The characteristic size of the observed solitons, unlike the variant in Ref. 55, is approximately half of (19) and is insensitive to the amplitude; the absence of an apparent relationship between the size of the vortex and its amplitude agrees with the variant in Ref. 73. b) The measured profiles of the Rossby soliton (see Fig. 8) are, on the one hand, in good agreement with the calculations based on the theory of Ref. 73, which reveals the effect of the soliton "memory" of the conditions of generation, owing to the presence of trapped particles, while on the other they disagree significantly with the variant in Ref. 55, which is distinguished by its analytic nature (continuity of the derivatives of the vorticity), but is a particular case (see Sec. 2.2). c) The observed scenarios of inelastic collisions of these vortices agree with the results of computational investigations,[42,98] in which, in accordance with the experiments discussed, the presence of a region of trapped particles of liquid in the soliton is taken into account. d) The velocity of propagation (drift) of the vortices is 1.2 times lower than V_R, determined by the formula (32), i.e., a factor of ~ 1.5 less than the theoretical value of the velocity of the soliton. This disagreement could be caused, in particular, by two factors: 1) the presence of some shift in the vertical component of the velocity owing to friction against the bottom and 2) the boundedness of the region of existence of the vortex in the meridional direction, owing to which $k_y \neq 0$ and the true theoretical value of V_R is less than that used in (12), where it is assumed in transforming from (7) that $k_y = 0$.

Thus the experimental data are in good agreement with the variant of the theory given in Refs. 73 and 98, and disagree substantially with the variant of Ref. 55. This should not be surprising, since, as indicated in Sec. 2.2, the probability of the experimental realization of such a particular solution, which has the form of a soliton of the type described in Ref. 55 (under the condition that particles of liquid are trapped), is apparently vanishingly small.

The experimental "surprises" described above are of a fundamental nature and stimulate the development of the theory.[73,98] It should be noted that the quantitative theory must also take into account the viscosity of the medium.

In connection with the comparison of experiment with theory, we also call attention to the result of a control experiment, performed in order to check the relations (11) and (13) for the drift velocity of vortices. In this (the only) experiment, unlike the experiments described thus far, the vessel was *exactly* paraboloidal, so that with a definite ("nominal") rotational velocity of the vessel all points on the equilibrium surface of the liquid are located at the same distance from the bottom Δz along the rotational axis. In addition, the thickness of the layer of liquid H (measured along the normal to the surface of the liquid) was a function of the point on the surface $H = \Delta z \cdot \cos\alpha$, and the Rossby velocity (11) equaled zero[21]:

$$V_R \sim \frac{\partial}{\partial y}\frac{\Delta z \cos\alpha}{\Omega_0 \cos\alpha} = 0.$$

Accordingly, the experiment showed that the Rossby vortex (observed by the procedure described above) with the vessel rotating with the nominal velocity stays in one place, when the vessel rotates with a higher velocity the vortex drifts westward, and when the vessel rotates with a lower velocity the vortex drifts eastward, in agreement with the theoretical relation, which is easily obtained from (33): $V_R \approx r_0 \Delta\Omega$, where $\Delta\Omega$ is the difference between the rotational frequency of the vessel and the nominal frequency, $r_0 = R_0/\sqrt{2}$ is the radius of the parallel along which the vortex drifts, and R_0 is the radius of the vessel.

Now that successful experiments on the generation and study of Rossby solitons have been performed, it would be interesting to try to realize an experimental steady-state soliton model of the Jovian Great Red Spot and other large-scale planetary vortices, self-maintained in a system of unstable oppositely moving zonal flows and existing for an arbitrarily long time, not limited by viscous and other losses of momentum. Experiments performed along these lines and the results of the theory are described in Sec. 4.

3.4. "Wave or vortex?" The vortex Rossby soliton—a wave solitary vortex

So, the Rossby soliton studied above is a "real" vortex, which efficiently transports particles trapped in it. On the other hand, the properties of this vortex—its character (cyclone-anticyclone asymmetry), dimensions, direction of drift, and drift velocity[22])—are predicted well and described well based on wave representations, according to which this vortex is a result of the mutual balancing of dispersion and nonlinearity (see Secs. 1.2 and 2.1). Thus the Rossby soliton is an explicitly dualistic object, and for this reason the following question often arises: "Is it a vortex or a wave?" This question is obviously not completely correctly posed. Such an object can be equally well called either a wave solitary (i.e., nondecaying) vortex or a vortex soliton—depending on which of its properties are being studied. The wave approach nevertheless appears to us to be more informative. In particular, fundamental phenomena such as the cyclone-anticyclone asymmetry can be explained simply only with its help, and in addition, by taking into account the wave motion in the vertical direction the two-dimensional soliton theory of the Jovian Great Red Spot can be markedly improved and the theory can be made to agree well with the observational data (see Sec. 5.1).

In this connection the English term "solitary vortex" [42] is apt, since it combines the concepts of a vortex and a solitary wave (soliton). As already indicated, in numerical studies[42] both the vortex properties of the structure under study (particle entrainment) and its wave or dispersive properties are taken into account—the existence of the structure itself is regarded as a consequence of the balance of dispersion and nonlinearity. (The fundamental effect of dispersion on the properties of dipolar (paired) Rossby vortices is also discussed in Sec. 8.)

4. GENERATION OF ROSSBY VORTICES (AND SOLITONS) BY OPPOSITELY DIRECTED ZONAL FLOWS (EXPERIMENT)

4.1. Formulation of the problem

The experiments described in the preceding section show that the experimentally observed Rossby soliton (anticyclone, whose dimensions are of the order of and greater than the Rossby-Obukhov radius, drifting along a parallel of the paraboloid opposite to the direction of global rotation) is very reminiscent of the vortex in the Jovian Great Red Spot (JGRS). This soliton, however, has a limited lifetime (~ 20 sec), determined by the viscosity of the medium. In order to realize the steady-state soliton model of the JGRS the Rossby soliton (generated, for example, by some source) must be placed into external flows, which would compensate the viscous (and, possibly, other) losses. In so doing, however, it is necessary to take into account the fact that the flows can play both a passive role (which is limited only to the "pumping" of the vortex) and an active role: they can manifest instability and generate their "own" vortices.[23] For this reason, at the first stage of the construction of a steady-state model of the JGRS it is necessary to study the question of the stability of the flows and, in particular, the possible relation between this question and the observed cyclone-anticyclone asymmetry of Rossby vortices.

It is clear that if the velocity profile of the flow is quite sharp, i.e., of the nature of a "tangential discontinuity" in the velocity, then the flow will be unstable (this, in particular, is the well-known Kelvin-Helmholtz instability), a consequence of which is vortex generation. In the presence of a cyclonic curl of the flow velocity (when the periphery of the liquid rotates faster than the vessel, while the center rotates more slowly) cyclones will be generated, while in the presence of an anticyclonic curl of the flows, anticyclones will be correspondingly generated. Under the indicated conditions the distinct cyclone-anticyclone asymmetry will be observed only in the case when the decrement of the experimentally observed decay of the cyclones is not less than the increment of their generation by the flows (otherwise the "pumping" of the cyclone by the flows could compensate its decay). But, as is well known,[100–106] the increment γ of the instability of oppositely directed flows depends on the steepness of their transverse gradient, more precisely, on the ratio between the characteristic size of the transverse gradient of the velocity of the flows δ and the size a of the generated vortex. Thus, under the conditions of the instability of the "tangential discontinuity," [24] i.e., when $\delta \ll a$, we have

$$\gamma \approx ku \approx \frac{u}{a}; \tag{41}$$

on the other hand, under conditions of a smooth flow profile, when $\delta \simeq a$, we have

$$\gamma \ll \frac{u}{a}. \tag{42}$$

As shown above (see Sec. 3.1.5) under the conditions studied, Rossby solitons decay over a time of the order of the transit time over one diameter of the cyclone, $2a/V_{dr}$. Therefore, if the velocity of the flows (exciting the vortices) is much higher than the drift velocity of the vortices,[25] then for $\delta \ll a$ the increment (41) will be much greater than the decay decrement of the cyclones, and the cyclone-anticyclone asymmetry will not appear, while when $\delta \lesssim a$, i.e., under the conditions (42), the growth increment of the vortex is insufficient to compensate the decay decrement of the cyclone and the cyclone-anticyclone asymmetry should be expected. (We note that this asymmetry was first observed experimentally[79,82,83,85,86] (see below), after which it was interpreted in the manner described here.)

4.2. Flows on incompressible shallow water with a free surface as a model of two-dimensional flows in a compressible medium. Landau's criterion of stability of a two-dimensional supersonic tangential velocity shear

In Ref. 107 L. D. Landau showed that a tangential velocity shear in a compressible medium becomes stable with respect to two-dimensional disturbances (in planes perpendicular to the plane of the shear) if the jump in the velocity Δu at the shear satisfies the condition

$$\Delta u \geqslant 2\sqrt{2}\, c_s, \tag{43}$$

where c_s is the velocity of sound. An analogous result was obtained by S. V. Bazdenkov and O. P. Pogutse[108] for a tangential shear in incompressible shallow water with a free surface:

$$\Delta u \geqslant 2\,(2gH_0)^{1/2}, \tag{44}$$

where g is the acceleration of gravity, H_0 is the thickness of the layer of "shallow water" (according to the definition of this term the quantity H_0 is much smaller than the wavelength λ of the two-dimensional perturbations under study). The equivalence of the results (43) and (44) is an illustration of the analogy[101] between two-dimensional gas dynamics and the theory of shallow water. In shallow water with a free surface the characteristic velocity of gravitational waves $(gH_0)^{1/2}$ plays the role of the velocity of sound, while rises and depressions in the surface of the incompressible liquid correspond to real compression and rarefaction in the compressible medium being modeled.

4.3. Experimental arrangement with oppositely directed zonal flows in a rotating paraboloid

The following method, illustrated in Fig. 12a, was used in experiments[82–88] to generate oppositely directed geostrophic flows in rotating "shallow water." Two wide ring-shaped slots, oriented along the parallels and separated from one another by some distance (l) along the meridian, are made in the thick bottom of a paraboloid. Zonal rings, which can freely rotate relative to the paraboloid in the plane of its bottom so that the angular velocities of this relative rotation of the rings are equal in magnitude and are mutually oppositely oriented, are inserted into these slots. An experiment in which the rings rotate independently of one another (Fig. 12b) will be described in Sec. 4.6. As they rotate, the rings entrain the layers of liquid lying above them, thereby creating oppositely directed zonal flows. By changing the distance l between the rings from one experiment to another it is possible to affect the real characteristic size δ of the trans-

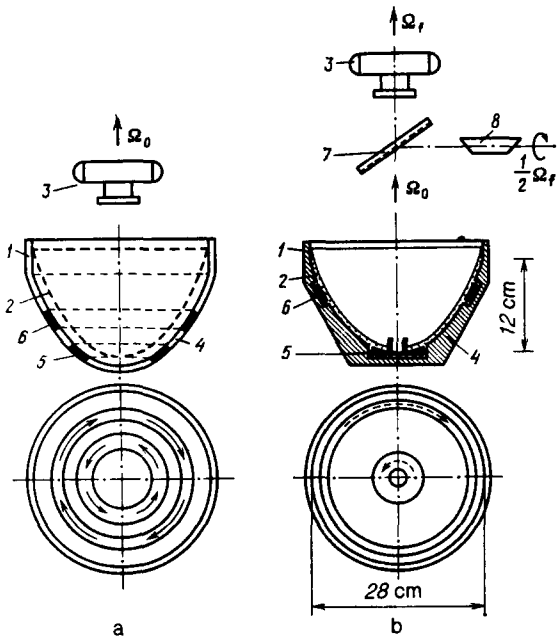

FIG. 12. a) Layout of the experimental arrangements[82-88] for generating Rossby vortices (solitons) with zonal flows. 1) Vessel with a parabolic bottom profile; 2) surface of the water, spreading out under rotation along the parabolic bottom; 3) camera rotating together with the vessel; 4) section of the (thick) bottom of a paraboloid, whose width was regulated from 1 mm (in experiments with a tangential shear in the flow velocity) to 3 cm (in experiments with a smooth flow profile); 5, 6) rotating rings, creating zonal flows with a velocity shear; the paraboloid rotates around the vertical axis counterclockwise with an angular velocity of Ω. In the view from above the solid arrows mark the anticyclonic direction of flow. b) Layout of experiment[87,88] in which a Rossby autosoliton was generated. 1, 2) Same as in a); 3) camera rotating together with the vortex; 5) section of the bottom of the paraboloid rotating faster than the vessel; 6) section of the bottom of the paraboloid rotating more slowly than the vessel; the distance between 5 and 6 along the meridian (width of the section 4 of the bottom of the paraboloid) equals 11 cm; 7) semitransparent mirror; 8) rotoscope: reflecting prism, rotating with an angular velocity of $\sim\Omega/2$ and enabling the observer to transform into a reference frame rotating with frequency $\sim\Omega$ and, in particular, making photographs in the reference frame of the vortex.

verse gradient of the velocity of the flows. We shall describe below the experiments on the excitation of vortices by flows with large and small (relative to r_R) l (and correspondingly δ). In the limit $l\to 0$, $\delta\approx H$; for $l=(2\text{–}3)H$, $\delta\approx l$; in addition, as H increases, δ increases and can exceed r_R; these conditions for generation of vortices by flows correspond to the relation (42); see Refs. 85 and 86.

4.4. Generation of chains of cyclones and anticyclones by oppositely directed zonal flows. Rossby solitons and the cyclone-anticyclone asymmetry

We shall first describe the results of experiments with a relatively large distance between the oppositely directed flows: $l\approx 3$ cm; in this case, $\delta\approx l\geqslant r_R$.[82,83,85,86] These experiments gave qualitatively different results depending on the sign of the curl of the oppositely directed flows. They showed that vortices (cyclones) of large size ($a>r_R$) are not generated when the curl of the flows is cyclonic (Fig. 13), while in the case of an anticyclonic curl large-scale vortices (anticyclones) are easily generated (Fig. 14). Thus with a relatively smooth transverse gradient of the velocity of the flows a distinct cyclone-anticyclone asymmetry is observed. It is easy to see that the circumstances under which it is observed correspond to the condition (42) (see Refs. 85 and 86 for a more detailed discussion).

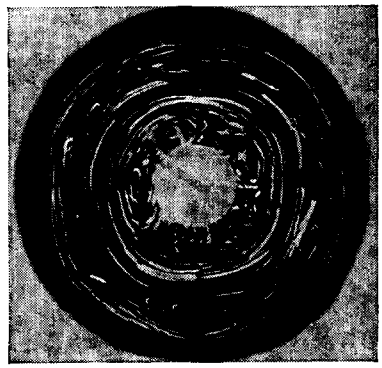

FIG. 13. Pattern of fluid flows with a smooth velocity profile and with a cyclonic vorticity of the oppositely directed flows.[82,83] Section 4 (see Fig. 12a) is 3 cm wide. The trajectories of white particles, floating on the surface of the water against the background of a black bottom, are shown.

The observed large vortices are steady-state in behavior, their diameter equals several Rossby-Obukhov radii, and they drift with a velocity approximately equal to the Rossby velocity relative to the paraboloid opposite to its direction of global rotation; their amplitude equals $h\approx 0.5$ and higher; they effectively transport particles of liquid. Based on all their properties as a whole these vortices can be regarded as Rossby solitons, which were described in Secs. 3.1.4–3.2.5. The number of vortices (m) on the perimeter of the chain is determined by the velocity of the flows: when the velocity is relatively low eight to ten anticyclones are observed, while for a relatively high velocity two to three anticyclones are observed (as in Fig. 14). We note that the interpretation of the chains described here of steady-state anticyclones as Rossby solitons corresponds to the theory of Ref. 109.

The decrease in the mode number m as the velocity of the flows increases is a fundamental characteristic, owing to which under other experimental conditions it is possible to form one Rossby autosoliton[87,88] on the perimeter of the system: $m=1$ (see Sec. 4.6).

We shall now examine the results of experiments with a small distance between the flows ($l\approx 1$ mm$\ll r_R$).[84–86,88] These experiments showed that practically the same effective generation of large-scale stationary vortices—both anticyclones (Fig. 15a) and cyclones (Fig. 15b)—occurs for both signs of the curl of the oppositely directed flows. Thus in this geometry of the experiment there is no cyclone-anticyclone asymmetry. This behavior also corresponds to the content of Sec. 4.2 [see the relation (41)].

The drift, geometric, and other properties of the observed anticyclones turn out to be the same as those of the anticyclones described in Sec. 3.1.4. As regards cyclones, in the presence of cyclonic flows they drift in the direction of

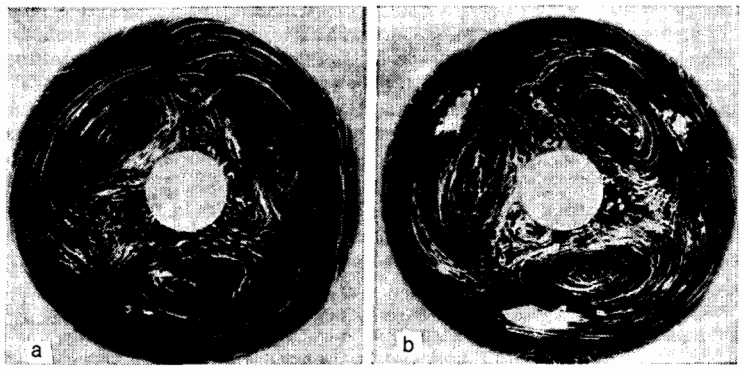

FIG. 14. Same as Fig. 13, under close experimental conditions, but with an anticyclonic vorticity of the oppositely directed flows.[82,83]

rotation of the paraboloid owing to the "bearing effect" pointed out in Ref. 110 which is unrelated to the β effect. There is a basis for assuming that the cyclonic Rossby vortices under study are not solitons: they are in a steady state, apparently, simply because they do not have time to decay as a result of the excessively effective "pumping" by the oppositely directed flows. Additional arguments in support of this conclusion will be presented in Secs. 4.6 and 8.2. (However, in the interpretation of the experiments under study with cyclones in flows and in the interpretation of the nature of the Jovian Brown Ovals (Sec. 5.2), it should be kept in mind that the theory admits the possibility of cyclonic Rossby solitons of a certain size in flows with a definite horizontal profile[42,57] or in the presence of vertical stratification.[53])

4.5. Disruption of the instability of a two-dimensional tangential discontinuity (Kelvin-Helmholtz) in the presence of a "supersonic" jump in the velocity of oppositely directed flows; agreement with Landau's criterion. Experimental illustration of the analogy between two-dimensional gas dynamics and shallow-water dynamics

The validity of the theoretical prediction, described by the relation (43) and (44), was studied experimentally using an apparatus of the type shown in Fig. 12a, in which the flows had a cyclonic curl (the periphery of the shallow water rotated more rapidly than the center) and were situated as close as possible to one another: the gap between them (the width of the Section 4) was only 1 mm wide—the "discontinuity" of the velocity. Experiments gave the following results. 1) If the relative velocity of the flows exceeds some threshold, then a Kelvin-Helmholtz (KH) instability, leading to the formation of a chain of vortices whose size λ along the surface of the water is always significantly greater than the depth of the liquid H_0 and the width of the discontinuity Δ, appears in the system. An example of such a chain—in the presence of a cyclonic curl of the oppositely directed flows—is shown in Fig. 15a. 2) If the relative velocity of the flows is greater than some higher threshold, then this instability does not occur. The magnitude of this second threshold corresponds well to the formula (44). This result is shown in Fig. 16. It is evident from Fig. 16a that when the velocity of the flows exceeds the second threshold, the vortices in Fig. 15a vanish (the broken line corresponds to increasing velocity, and the solid line corresponds to decreasing velocity). The right side of the figure shows that when the depth of the liquid H_0 changes the second threshold velocity changes $\sim (g^* H_0)^{1/2}$ in accordance with the theoretical result.[107,108,26]

Thus in this section we have given a graphic illustration of the remarkable analogy between two-dimensional gas dynamics and the dynamics of shallow water with a free surface. This analogy enables laboratory simulation not only of planetary atmospheric vortices (described in this review), but also—under different experimental conditions—of the hydrodynamic mechanism of generation of the spiral structure of galaxies, which have a jump in the velocity on the rotational profile (see Sec. 6).[27]

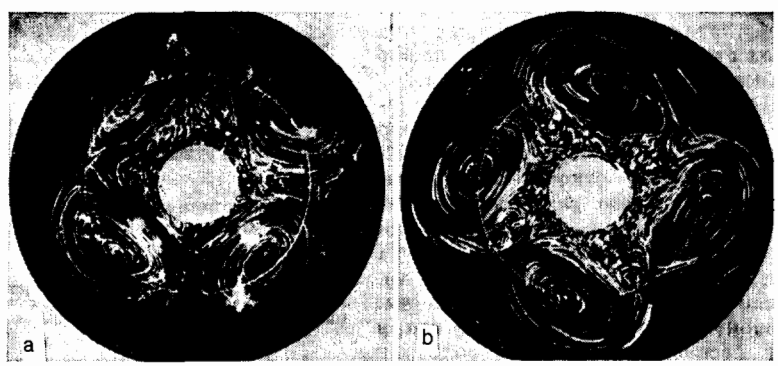

FIG. 15. Pattern of the fluid flows with a sharp velocity profile of oppositely directed flows. Section 4 (see Fig. 12a) is 1 mm wide. a) Cyclonic vorticity; b) anticyclonic vorticity.[84–86] The white circle is the line of "discontinuity" of the velocity of the flows.

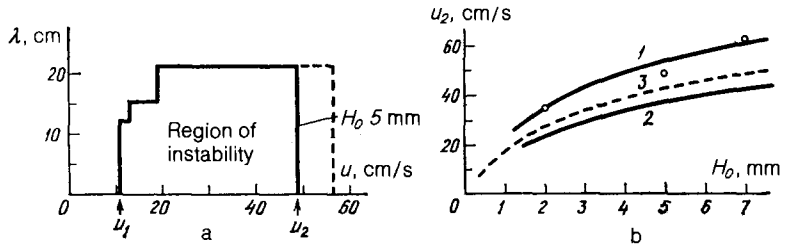

FIG. 16. a) The azimuthal size of the vortices λ as a function of the velocity of the flows, measured at the location of the discontinuity on the surface of the water under the conditions of Fig. 15. b) The threshold u_2 at which the instability of the tangential shear vanishes as a function of the depth of the liquid. 1) Velocity of the rings moving the water lying above them; 2) velocity of flows on the surface of the liquid; 3) theoretical[108] velocity of the flows $u = (2g^*H_0)^{1/2}$ (the relative velocity of the flows equals $2u$).

4.6. Rossby autosoliton—self-organization in zonal flows

Searches for a Rossby autosoliton—a single, on the entire parallel of the paraboloid, and nondecaying anticyclonic vortex, "fed" by the oppositely directed flows—were initiated immediately after the successful experiments[78–81] described in Secs. 3.1 and 3.2. The problem was formulated as follows: after a soliton is generated by some source (for example, a "pumping disk") try to compensate its viscous momentum losses, by utilizing for this oppositely directed flows. In this case, the fundamental condition was that the experiment had to be confined to a flow regime in which the velocity of the flows is quite low and the flows are stable. Such a regime was necessary in order for the flows to play a purely "energetic" role, feeding the soliton, but without generating their "own" vortices. The first experiments were performed on the experimental arrangement described in Secs. 4.3 and 4.4 with the distance between the flows $l = 3$ cm (see Fig. 12a). They gave a negative result: it turned out that the inclusion of the flows destroys the soliton. This meant that under the conditions of this geometry the profile of the flows cannot be matched with the profile of the soliton.

After a considerable time, during which the above-described characteristics of cyclogenesis by flows moving in opposite directions with a high velocity were studied, the search for the autosoliton was continued on an experimental arrangement with a larger distance between the flows: $l = 11$ cm (see Fig. 12b). The experiments showed that it is possible to establish a rotational regime of the zonal rings and the paraboloid in which the Rossby soliton, generated by the "pumping disk," is not destroyed by the oppositely directed flows and is slightly fed by them; the lifetime of the soliton, however, increases insignificantly. After this, the experiment was modified: the pumping disk was removed completely, and the zonal rings were made to be independent of one another. The experiment[87,88] showed that there exists a regime in which quite fast oppositely directed flows which have an *anticyclonic curl* of the velocity generate a nondecaying large-scale Rossby soliton, the only one on the perimeter of the paraboloid and self-organized in the system of flows. (In the presence of a cyclonic curl of the flows the large-scale vortex is not generated—in accordance with the result of Sec. 4.4 regarding the cyclone-anticyclone asymmetry.)

Figure 17 shows photographs of the autosoliton (they were made using a camera rotating together with the vortex, unlike the previously presented photographs, which were made with a camera rotating together with the paraboloid). The parameters of the vortex demonstrated in Fig. 17 (size, amplitude, direction and velocity of drift and intrinsic rotation) are characteristic of the Rossby soliton described in Secs. 3.1 and 3.2. In particular, the diameter of the vortex is $2a \approx (3\text{–}4)r_R$, its amplitude is $h = \Delta H/H_0 \approx 1$, the streamlines in the core are closed, and it effectively transports trapped particles (see Fig. 17).[28)] This vortex is a result of self-organization of the soliton structure in a system of oppositely directed flows: when the vortex appears, the profile of the flows radically changes, adjusting itself so as to be matched with the vortex (Fig. 18). Another important property of the autosoliton described is that its vorticity (the curl of the velocity) is several times larger than in the surrounding flow,[87,88] analogous to what happens in large vortices in the atmospheres of large planets.[63] The observed autosoliton can be regarded as a steady-state one: its lifetime is infinite, though in time it goes through a deformation of an oscillatory character, transforming, for example, from a realization of the type shown in Fig. 17a to the one shown in Fig. 17b.

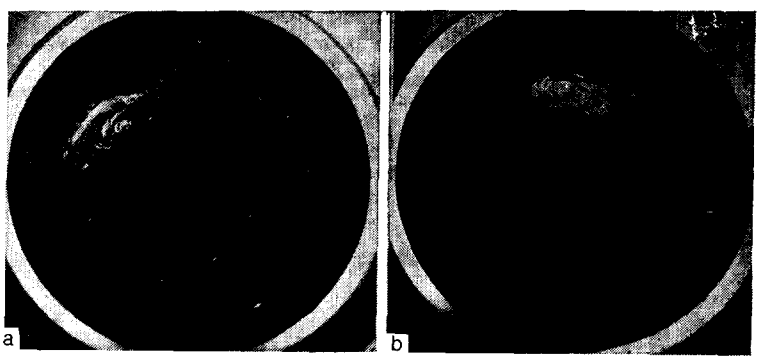

FIG. 17. Rossby autosoliton with several different flow velocities (anticyclonic vorticity).[87,88] The camera rotates together with the vortex (and not together with the vessel, as in the preceding photographs).

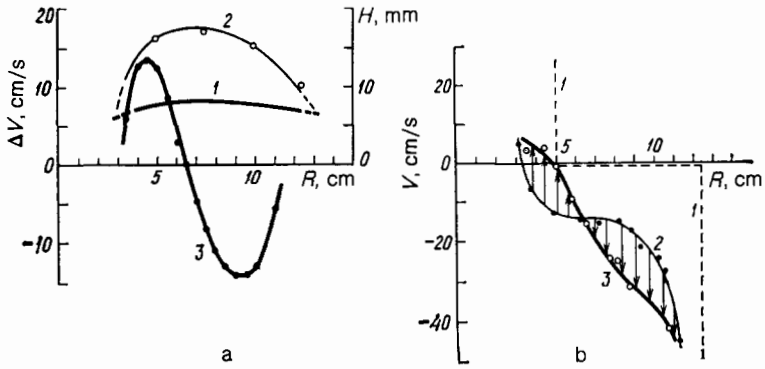

FIG. 18. a) Depth profiles of the liquid in the meridional section of the rotating paraboloid: the depth of the liquid as a function of the distance to the axis of rotation[87,88]; 1) in the region diametrically opposite to the vortex; 2) in the region of the vortex; curve 3 shows the profile of the velocity in the vortex; the velocity is measured relative to the flow, as indicated by the arrows in Fig. 18b. b) Profiles of the linear azimuthal velocity of particles on the surface of the liquid in the system of the rotating vessel: 1) in the absence of a vortex; 2) in the vortex generation regime in a region diametrically opposite to the vortex; 3) inside the vortex.

The Rossby autosoliton studied here is a result of the development of an instability of oppositely directed flows in the mode $m = 1$. Other modes of this instability are also observed, and their number is the higher the lower is the velocity of the flows—in agreement with the data in Secs. 4.4 and 4.5. Examples of modes with $m > 1$ and the manner of their alternation as the velocity of the oppositely directed flows increases are illustrated in Figs. 19 and 20. It is important to note that, as experiments show, the fewer are the vortices in the chain, with other conditions being equal, the larger is their amplitude and the stronger is their localization. Comparison of Figs. 17, 19, and 20 with the results of Sec. 4.4 shows that the previously described anticyclonic vortex structures (see Fig. 14) consist of a chain of Rossby autosolitons, generated in the mode $m = 3$ by the hydrodynamic instability of the oppositely directed flows.

The spatial localization of the structures studied, naturally, is a result of their strong nonlinearity. One indicator of this nonlinearity is the ratio of the rotational velocity of the particles in the vortices to the drift velocity of the vortices. This ratio, as shown above, is much greater than one, which gives rise to the effective transport of liquid by the vortex.

The planetary aspect of the results described here is studied in Sec. 5.

In order to identify the instability that generates the Rossby autosoliton in the most interesting state of the $m = 1$ mode (see Fig. 17), we shall turn our attention to one more important fact. In this state, the outer ring rotates (opposite to the direction of rotation of the paraboloid) with an angular velocity approximately equal to $2\Omega_0$. At the same time, the velocity of the interior flow is $u = 2\Omega_0 r_0 \approx 300$ cm/s and the Mach number is $\mathrm{Ma} = u/(g^* H_0)^{1/2} \approx 7.5 > 2\sqrt{2}$, even for $H_0 = 1$ cm. Therefore the jump in the velocity at the discontinuity of the external flow satisfies the criterion (44) for the disruption of the Kelvin-Helmholtz instability. Together with the fact that under the conditions of a cyclonic curl of the vortices (when the periphery of the vessel rotates with a higher angular velocity than its center) large vortices are not excited, this indicates that an autosoliton is generated in the experiment under study apparently because of the centrifugal instability (CI). This is the instability which under certain conditions remains in a differentially rotating liquid even when $\mathrm{Ma} \gg 1$, if its center rotates more rapidly than the periphery. Under the experimental conditions of Refs. 89–91 and 123a this instability simulates in the laboratory the probable hydrodynamic mechanism of the formation of the spiral structure of galaxies, whose rotation profile exhibits a jump in the velocity (see Sec. 6).[29] Here it should be emphasized that the "supersonic" values of the Mach number Ma obtained in this experiment with the Rossby autosoliton should by no means be regarded as necessary: they are a consequence of the geometry chosen for the experiment. This is indicated by data from experiments performed on three variants of the experimental arrangements described here with different distances (l) between the oppositely moving flows. These experiments showed that the relative velocity of the oppositely directed flows u, required for

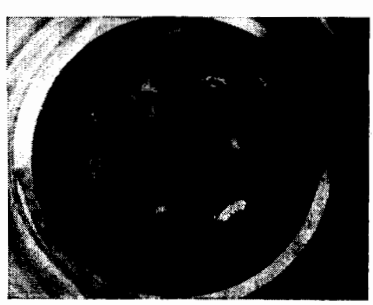

FIG. 19. Chain of autosolitons in the mode $m = 3$. It is evident that the vortices are very distinctly localized.[88]

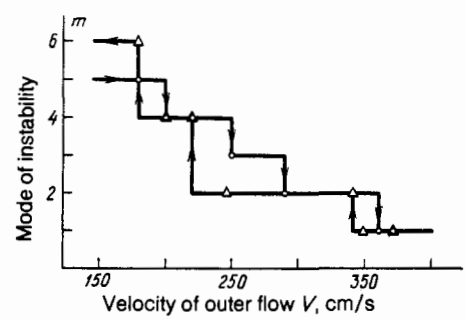

FIG. 20. The mode number m as a function of the velocity of the ring generating the outer flow in the geometry of Figs. 12b and 17.

exciting a chain of vortices in a given mode m, increases as Ω_0, H_0, and l increase, so that this corresponds to the following behavior. The differential in the velocity of the flows over the size of the vortex (ua/l) must ensure a velocity of rotation of the flow which substantially exceeds the drift velocity $\sim V_R$; it is precisely in this case that we see a vortex with a distinct region in which particles are trapped (see Fig. 17). This rule has the form

$$u \approx \frac{cV_R l}{r_R} \approx \frac{c\Omega_0^2 l H_0^{1/2}}{(g^*)^{1/2}}, \tag{45}$$

where the coefficient c is of order of unity and depends on the details of the experiment. It is evident from here, in particular, that for the large value of l chosen in the experiments on the generation of an autosoliton, Mach's number $\mathrm{Ma} = u/(g^* H_0)^{1/2}$ is comparatively large.

This, however, does not give rise to any fundamental difficulties in the modeling of real atmospheric vortices, for which $\mathrm{Ma} < 1$ always holds. The point is that, as will be shown in Sec. 5.3, in studying vortices occurring in nature the three-dimensionality (baroclinicity) of the wave motion must be taken into account; in this case the Mach number Ma, proportional to V_R, decreases by several factors of ten and equals the "true" value of Ma.

4.7. Why are the observed structures nevertheless Rossby vortices?

The question posed stems from the fact that chains of vortices, which superficially are similar to those shown above (see Figs. 14 and 15), are also observed in completely different experimental situations, unrelated either to the Rossby regime [see (3)] or, to a lesser extent, to the conditions of generation of Rossby vortices. We shall present some examples. One example is the experimental study[110] of the Kelvin-Helmholtz instability in oppositely directed concentric jets of gas. According to the intention of the authors, it is conducted under conditions when the oppositely directed flows are almost symmetric relative to the laboratory system of coordinates, which is thus practically inertial; hence the centrifugal and Coriolis forces can be neglected and, therefore, the conditions of the experiments of Ref. 110 are not those of the Rossby regime (see Sec. 1.1). In addition, in Ref. 110 $\mathrm{Ma} \to 0$. Very effective generation of vortex chains is demonstrated in Refs. 111 and 112, which simulate polar cyclones on earth. In them, the oppositely directed flows are generated by the action of the Coriolis force on the forced pumping of liquid in the rotating ring layer. The most effective generation of steady-state vortices occurs under conditions when the liquid is pumped along the edges of the ring-shaped gap and coalesces at its center (where eddies thus form); it is easy to see that cyclones are generated for this direction of motion of the liquid. In this system the β effect is virtually absent (the vortices have almost no dispersion).

It is now not difficult to verify that the conditions of the experiments on the generation of Rossby vortices (solitons), studied in Sec. 4.4, differ radically from the conditions of the experiments cited in this section. The differences are attributable to two circumstances. 1) In this review, structures which are larger than the Rossby radius ($a > r_R$ or $a > r_i$) are studied, unlike Refs. 111 and 112 where $a < r_R$. In other words, the approximation adopted in the review is equivalent to the approximation of a magnetized plasma, where the scale of the structures is larger than the Larmor radius of the ions (analogous to the Rossby radius). 2) The properties of the vortices (solitons) studied here are fundamentally determined by the dispersion of the Rossby waves (i.e., the β effect). A consequence of this is the distinct dispersion-nonlinear effect, such as the cyclone-anticyclone asymmetry in the Rossby regime. This asymmetry is observed both in the state of "free transit" of the vortices and under conditions when they are generated in a steady-state manner by unstable flows with a smooth (compared with r_R) velocity profile. It is expressed, in particular, in the fact that the anticyclonic autosoliton exists (Sec. 4.6), while the cyclonic one does not exist. If, on the other hand, the flows have a sharp velocity profile, then the cyclone-anticyclone asymmetry vanishes, and the differences in the conditions of generation of the vortices studied in this review and of the vortices studied in Refs. 110–112 are no longer fundamental: the vortices are effectively generated irrespectively of whether or not they are (like here) or are not (like in Refs. 110–112) Rossby vortices. The conditions under which vortices are generated by flows with a smooth profile are characteristic for large atmospheric vortices on large planets (Jupiter and Saturn), while the regime with the sharp profile is characteristic for planetary vortices in the earth's atmosphere; in the last case, the cyclone-anticyclone asymmetry does not occur, which is in good agreement with what was said above (the effect of the rotation of the system and the β effect on the instability of shear flows is discussed in Ref. 113).

5. ROSSBY SOLITONS AND PLANETARY VORTICES

As already noted,[7,10,18,44] Rossby waves can substantially determine the large-scale cyclogenesis processes occurring in the oceans and in planetary atmospheres. Here we shall study this question in greater detail, primarily in application to the large planets Jupiter and Saturn, since on these planets the prerequisites for the soliton concept under study are realized, namely, 1) the dimensions of the vortices are greater than the Rossby radius ($a > r_R$ or $a > r_i$)—the "magnetized plasma" approximation; 2) the ratio of the radius r_R to the radius of the planet R is a small parameter. On the indicated planets $r_R = 6000$ km (at the latitude of the JGRS), $R = 70\,000$ km, $r_R/R \lesssim 10^{-1}$. In this sense the earth is less convenient for analysis, since in its atmosphere $r_R \approx 3000$ km (at middle latitudes) and $r_R/R \approx 1/2$—this parameter is no longer small. For this reason, we shall not study terrestrial vortices here—we refer the reader to Refs. 11, 111–113. With regard to the atmospheric vortex structures studied, we adopt the "shallow water" concepts. A detailed discussion of the justification for this approach is given in Ref. 117.

5.1. Experimental soliton model of the Jovian Great Red Spot

As shown above (see Sec. 3), the Rossby soliton, observed in experiments of Refs. 79, 82, 88 can in principle be regarded as a laboratory model of the vortex (JGRS), which

qualitatively supports the existing soliton theory of this natural phenomenon. This concept is further supported by the above-described (see Secs. 3.1.5 and 4.4, 4.6) experimental results, demonstrating the cyclone-anticyclone asymmetry of Rossby vortices, which is observed in two distinct phenomena: 1) anticyclones are stable and are distinguished by their comparatively long lifetime; cyclones decay comparatively rapidly (disperse); 2) the oppositely moving zonal flows with a smooth transverse gradient of the velocity (for example, such as those in the region of the JGRS, where the characteristic transverse size of the flow profile exceeds r_R) generate only anticyclones[82,83,85–88]; in other words, oppositely directed flows with a smooth gradient of the velocity generate a large-scale (greater than r_R) planetary vortex only when they have an anticyclonic curl of the velocity. This experimental behavior has an analogy in the Jovian atmosphere. Indeed, as observations show,[61] the vortex in the JGRS is an anticyclone and exists in the region of zonal flows (see Fig. 3, point A), where their velocity curl is anticyclonic. In addition, in the neighboring region (see Fig. 3, point B), where the amplitude of the flows is even higher but their curl is cyclonic, there is no large vortex (!). Thus there is a clear parallel between the phenomena observed in nature and in the laboratory.

Two experimentally observable modifications of the Rossby soliton were described above (Secs. 3.1 and 4.6): in one the soliton lifetime is limited by the viscosity of the medium (and equals ~ 20 s), while in the other—the autosoliton state—the lifetime is not limited at all. These modifications can be regarded as two soliton models of the vortex in the JGRS: the first as a nonsteady-state and the second (Rossby autosoliton) as a steady-state model of the Jovian Great Red Spot. The second model, of course, conforms more closely to natural conditions (see the next section).

5.2. Why is there only one vortex "Jovian Great Red Spot" along the entire perimeter of the planet?

A simple and natural explanation of the intriguing question of why this natural vortex is the only vortex along the entire perimeter of its parallel (or, in other words, what prevents the existence of another such vortex at another location on the perimeter?) can apparently be found on the basis of the experimental steady-state soliton model of the JGRS examined in the preceding section. The answer to this question lies in the fact that the JGRS is simply the first (and quite localized) mode of the hydrodynamic instability of oppositely directed zonal flows. It is characterized by the number of vortices along the perimeter $m = 1$ and develops in the presence of a jump in the velocity of the flows and for a flow profile for which the existence of second and higher order modes ($m > 2$) i.e., a chain of vortices, corresponding to a shorter wavelength of the instability, is excluded.

In order to imagine the probable mechanism of the phenomenon, let us assume that as the oppositely moving directed flows are formed their velocity gradually increases. Then, as is evident from Figs. 17, 19, and 20, the modes of instability of the flows will change successively: every subsequent (larger scale) mode, as it appears, will suppress the preceding (smaller scale) mode. For this reason, in particular, when an autosoliton appears at the largest mode $m = 1$, corresponding to the longest wavelength of the instability (a single vortex along the perimeter of the system), the shallower water $m = 2$, corresponding to a shorter wavelength of the instability (two vortices along the perimeter), will vanish. This change in modes is linked with such a restructuring of the flows (accompanied by a widening of their profile) which occurs, in particular, when the mode $m = 1$ appears and which corresponds to the steady state of the mode $m = 1$, but excludes the existence of the mode $m = 2$ and shorter wavelength modes.

Thus, in the final analysis, the uniqueness of the JGRS vortex over the entire perimeter of its parallel is explained by the fact that in the region of this parallel the zonal flows have a quite wide velocity profile along the meridian. For narrower profiles chains of vortices are possible (as happens, for example, on the latitudes of the White and Brown Ovals; see below). It is entirely probable that the observed profile of zonal flows at the latitude of the JGRS was established not without the influence of this vortex itself. In addition, the circumstance that the mode $m = 1$ occupies a small part of the entire perimeter of the planet (the region of trapping of the particles in the JGRS extends over about 25 000 kilometers, which is appreciably shorter than one-tenth the perimeter of the planet) is explained by the strong nonlinearity of the vortex; the index of this nonlinearity—the ratio of the characteristic rotational velocity of the vortex to its drift velocity—equals about 20 in the JGRS.

We note that the experimentally observed fundamental phenomenon of the successive change of modes of the shear instability, leading to the evolution of oppositely directed flows into a system with one autosoliton, has still not been explained theoretically. (The mechanism of the change in modes of the instability is discussed in greater detail in Sec. 7.1.)

The steady-state behavior of the vortex of the JGRS, which has already been observed for 300 years, is explained by the equilibrium established between the increment of the hydrodynamic instability that "untwists" the vortex and its damping decrement. The physical *quasi-two-dimensionality* of the vortex under study and analogous vortices in the atmospheres of Jupiter and Saturn is indicated, in particular, by the fact that all large long-lived vortices on these parallels are observed at the center between the oppositely directed flows (at the points A and C in Fig. 3), where the *horizontal* gradient of the velocity of the flows is maximum. In this respect, an important result of astronomical observations is described in Ref. 61: the condition of instability of zonal flows is satisfied on the latitude of the JGRS vortex (as well as on the latitudes of localization of other large vortices on Jupiter and Saturn; see below). This condition, according to which its vorticity must have a maximum value on the flow profile[103–105] (generalized Rayleigh criterion[100–102]), has the form[44,83,105]

$$\frac{\partial^2 u}{\partial y^2} r_R^2 - (V_R + u) = 0, \tag{46}$$

where u is the velocity of the flow (positive toward the east), y is the coordinate along the meridian (positive toward the

north), and V_R is the absolute magnitude of the Rossby velocity.

The pumping of the JGRS vortex by zonal flows[114,115] is apparently responsible for its prolonged existence; in the absence of pumping the vortex would probably decay within a few years, as a result of either of two independent processes: viscous damping with the decrement (47) and nonviscous damping with the decrement (22). Using the classical value of the coefficient of viscosity,[116] setting the effective height of Jupiter's atmosphere in the region of the JGRS equal to $H_0 \approx 25$ km (see Sec. 5.3), $\Omega_0 \approx 10^{-4}$ s^{-1}, and setting the viscous damping time (τ) of the JGRS equal to the corresponding estimate for the Rossby vortex on a solid underlying surface,[24] we obtain

$$\tau \approx H_0 (\nu\Omega_0)^{-1/2} \approx 10 \text{ years}. \quad (47)$$

An estimate based on the decrement (22) gives a significantly shorter lifetime of the vortex. Therefore the assumption that the steady state of the JGRS can exist only under the condition of quite intense pumping of the vortex by zonal flows appears to be realistic.

Thus the Rossby autosoliton described in Sec. 4.6, for the first time models *simultaneously all three* intriguing properties of the natural vortex in the Jovian Great Red Spot, namely, 1) steady-state behavior, 2) self-organization in zonal flows, and 3) being the only vortex along the entire perimeter of the planet.

The experimental Rossby autosoliton has another property, analogous to one observed in the Jovian vortices: the vorticity in it is much higher than the vorticity in the surrounding flow.[87,88] Thus an experimental soliton model has been created for the first time which apparently no longer leaves any doubts about the fact that it qualitatively models the nature of this planetary vortex (and other similar vortices). In order to compare the external view of the natural vortex of the JGRS with its laboratory model, Figure 21 shows a photograph of the JGRS (southern hemisphere on Jupiter, 22 °S.L.), taken from the jacket of Ref. 1a. The size of the vortex along the parallel is about 25 000 km (along the region of trapped particles) and oppositely directed turbulent (zonal) flows with an anticyclonic curl of the velocity flow around it from the north and the south. The similarity between Fig. 21 and Fig. 17 is evident.

The fact that the experimental model studied is two-dimensional and therefore cannot give an exact quantitative correspondence with the astronomical observations must, however, be taken into account. For this reason, we shall briefly describe the three-dimensional approach to the soliton model of the JGRS.

5.3. Three-dimensional soliton model of the Jovian Great Red Spot

It turns out that good agreement (not only qualitative but also quantitative) between the soliton model under study and the data from astronomical observations can be obtained simply by taking into account[44,60] the wave motion in the Rossby soliton along the vertical coordinate.

According to Voyager data[61,69] the JGRS vortex in the upper atmosphere of Jupiter is an anticyclone with a relative amplitude of $h \approx 10^{-1}$, "floating" along the parallel at a latitude of $-22°$ in an approximately isothermal cloud layer with an effective thickness of $H_0 \approx 20$ km (this quantity characterizes the decay of the atmospheric density along the vertical by a factor of $1/e$; the total thickness of the layer can be several times greater than H_0). This layer is physically distinguished by the fact that the temperature reaches its lowest value— -130 K—as a function of altitude in it (the average pressure in the layer equals about 1/3 of the pressure on earth). Beneath this cloud layer, beginning at a level where the gas pressure is only one-half the pressure in the earth's atmosphere, a gaseous substratum, in which the pressure varies with altitude according to the adiabatic law, extends deep into the interior of the planet: in this medium the Brunt-Väisälä frequency equals zero [see the discussion for (17)], so that some authors[62] think that the top boundary of this substratum in corresponding models may be regarded to be a solid surface.

Jupiter's rotational period is about ten hours, the acceleration of gravity is $g \approx 2.5 \cdot 10^3$ cm/s^2, and the planet's radi-

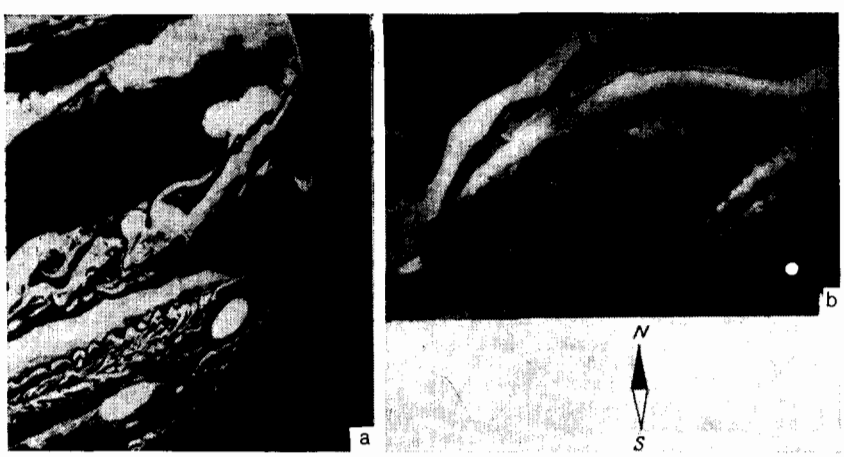

FIG. 21. Vortex in the JGRS in the Jovian atmosphere (southern hemisphere)—see photograph 12.4 and jacket of Ref. 1a. The dark oval at the center of the right side of Fig. 21a is the JGRS, the white ovals lie to the south and to the west. Figure 21b shows the JGRS in an enlarged scale.

us is 70 000 km. The vortex drifts westward along the parallel at a latitude of $-22°$ with a velocity of about 3 m/s and rotates around its axis opposite to the direction of rotation of the planet with a characteristic period of about one week. The Rossby-Obukhov radius for the JGRS equals $r_R \approx 6000$ km, and the Rossby velocity (11,12) $V_R \approx 160$ m/s (Table II).

According to the two-dimensional soliton model of the JGRS the drift velocity of this natural vortex must exceed $V_R \approx 160$ m/s, while in reality it equals about 3 m/s, i.e., approximately 50 times lower than V_R. Therefore the two-dimensional (barotropic) soliton model of the JGRS, being in quite good *qualitative* agreement with the observational data, is not in *quantitative* agreement.

For this reason, we shall now consider the baroclinic model,[44,60] for which we shall taken into account the possibility of wave motion in the vortex along the vertical, associated with the variability of the density of the medium as a function of height in the atmosphere—analogous to the manner in which this is done in the analysis of synoptic vortices (see Sec. 1.4). Then, as already pointed out, the dispersion equation for Rossby waves will admit the existence of not only a two-dimensional (barotropic) mode, but also three-dimensional modes, more accurately, quasi-two-dimensional (baroclinic) modes, in which the wave number along the vertical $k_z \neq 0$. We shall now assume[44,60] that the soliton solution, analogous to the two-dimensional model, also exists in the baroclinic mode indicated here. Then, according to Sec. 1.4, the "baroclinic" (or internal) Rossby radius r_i will appear in all expressions for the parameters of the soliton instead of the "barotropic" radius r_R, which is much larger than r_i. Such a baroclinic soliton solution was studied, in particular, in Ref. 70 and also in Ref. 42 [in the latter, the complete necessary procedure is not carried out, and the transition from the barotropic mode to the baroclinic mode is made simply by replacing the actual acceleration of gravity g by some equivalent value $g' \approx (1/15)g$[30]; in addition, the scale r_R is replaced by $r_1 \approx r_R/4$]. The baroclinic radius r_i can be estimated with the help of the relations (16) and (17). In so doing, for the case of an approximately isothermal atmosphere and the vertical mode with an effective wave number $k_z \approx \pi/H$,[31] we obtain the relation[44,60]

$$\varepsilon \equiv \frac{r_R}{r_1} \approx \pi \left(\frac{\gamma}{\gamma-1}\right)^{1/2}, \tag{48}$$

where $\gamma \approx 1.4$ is the adiabatic index. Now, with the help of (8) and (12), it is not difficult to see that when r_R is replaced by r_i the size of the soliton decreases by a factor of $\varepsilon \approx 6$, while the drift velocity of the soliton decreases by a factor of $\varepsilon^2 = 36$. This means that the characteristic radius of the JGRS must equal several r_i, i.e., several thousands of kilometers, as is in fact the case in reality. This means also that the drift velocity of the JGRS must equal approximately 4.5 m/s, which is close to the observed velocity. It is evident that both approaches[42a,44] (and they admit obvious quantitative variations within the limits of the indicated order of magnitude of the quantities) give qualitatively close results.

Thus the baroclinic model (to which it is better to refer not as a three-dimensional model, but rather as a quasi-two-dimensional model), unlike the barotropic (two-dimensional) model, is in good quantitative agreement with the astronomical observations; this supports the viewpoint that the

TABLE II. Large long-lived vortices in the atmospheres of Jupiter and Saturn (the last lines are combined).

Planet	Latitude	Name of vortex	Sign of vorticity of the vortex	Observed lifetime, years	Diameter along the meridian (parallel), thousand km	Drift velocity, m/s	Direction of drift	References
Jupiter	22° S.L.	Great Red Spot (GRS)	Anticyclone	More than 300	13×26***	3	Westward	38
	34° S.L.	White Ovals (WO)	Anticyclones	More than 45	5×7	4	Eastward	38
	14° N.L.	Brown Ovals ("barges")	Cyclones*	More than 2.5	1.5×7.5	2.5	Eastward	65, 68
Saturn	75° N.L.	Big Bertha	Anticyclone	More than 1**	5×7			69
	42° N.L.	Brown Spots (BS)	Anticyclones	More than 1**	3.3×5	5	Same	69
	27° N.L. 55° S.L.	UV spots; Anne's Spot (AS)	Anticyclones	More than 1**	~3; ~3.	;30	Eastward	69

*With this single exception all large vortices are anticyclones. The cyclones of Jupiter and Saturn are usually not larger than 1000 km and their lifetime is not longer than one week.[68]

**The observations began only recently.[69]

***The dimensions of the region of trapping of the particles are indicated.

JGRS vortex is a Rossby soliton. (We note that unlike Refs. 44, 60, and 88, here we do not examine the variant of the soliton model of the JGRS given in Ref. 55, in view of the fact that, as is now clear (see Secs. 2.2 and 3.3), this variant has a very low probability of being realized.)

Another quantitative difference, associated with the value of the Mach number, between the autosoliton model of the natural JGRS vortex studied here and the object being modeled was already discussed in Sec. 4.6. Just as the difference associated with the two-dimensionality of the model, it is not a fundamental one, since it disappears when the wave motion along the vertical is taken into account.

We note that what has been said here and previously about the properties and nature of the JGRS vortex is also true for other large (though smaller) anticyclonic vortices in the Jovian atmosphere—the so-called White Ovals, which appeared in 1938 as a result of a strong disturbance of Jupiter's atmosphere.[36–38] Other planetary vortices are discussed in the next section.

5.4. Other large vortices in the atmospheres of large planets

The main properties of all large vortices on Jupiter and Saturn have the following characteristic features.[44,117] 1) Cyclone-anticyclone asymmetry. With one exception, which only confirms the rule (the Brown Ovals, or "barges," of Jupiter at 14 °N.L.), all large long-lived vortices on large planets are anticyclones. 2) The hierarchy of scales and lifetimes of the vortices (the dimensions of the vortices are of the order of the Rossby radius r_i or larger). The largest vortex—the JGRS—has the longest lifetime ($\tau > 300$ years). The lifetimes of smaller vortices are substantially shorter. 3) The drift of the vortices along the parallels. All large vortices drift around the axis of the planet. Thus the JGRS vortex drifts westward, while the Brown Ovals drift eastward. 4) The characteristic rotational frequency for all large vortices is lower than the rotational frequency of the planet. 5) The linear velocities of the particles in the vortices are substantially higher than the drift velocity—the vortices effectively entrain particles of the medium contained in them. 6) All anticyclones are observed in regions of zonal flows where the curl of the velocity is anticyclonic, while the transverse velocity gradient is smooth. 7) The cyclonic "barges" of Jupiter are observed in the region of the cyclonic curl of the velocity of the flows, which have a sharp meridional gradient.[68] The differential of the velocity of the flows in the region of the "barges" equals about 125 m/s over a distance of about only 1.5 thousand kilometers, while in the region of the JGRS it is several times smaller. 8) All large vortices are localized in regions of zonal flows where the horizontal gradient of the velocity of the flows is maximum (i.e., the centers of the vortices lie near the transition of the velocity of the flows through zero). 9) At latitudes corresponding to all large vortices on Jupiter and Saturn the criterion of hydrodynamic instability of the zonal flows, corresponding to (46), is satisfied.

Based on everything said above, the set of enumerated properties of anticyclonic planetary vortices makes it possible to regard them as Rossby vortices, generated by unstable zonal flows. As regards the cyclonic "barges" of Jupiter, according to Sec. 4.4 they are apparently noncharacteristic modes and exist only owing to the intensive "pumping" by flows with an extremely sharp transverse gradient of the velocity—in accordance with (41). Under conditions under which these vortices are observed, the cyclone-anticyclone asymmetry should not occur, as shown in Secs. 4.1 and 4.4. We recall that the Rossby autosoliton, the only one on the entire perimeter of the system, can be created experimentally only in the form of an *anticyclone* (see Sec. 4.6).

The cyclone-anticyclone asymmetry is also observed in the oceans on earth. According to numerous observations (see, for example, Refs. 19b, 19a (p. 218), and 118–120) at depths of several hundreds of meters, very long-lived baroclinic vortices, having the forms of "lenses," occur (excited by appropriate sources) at the boundary between layers with different temperatures. They are *monopolar* vortices, as a rule *anticyclones*, and their horizontal dimensions are somewhat greater than the internal Rossby radius r_i. These structures can be regarded as "candidates" for Rossby solitons.[73] It is interesting to note that the vertical structure of these anticyclones—in accordance with the multilayer model of Ref. 19a—can be thought of as a baroclinic mode of the envelope with an effective vertical wave number $k_z \approx \pi/H_0$, where H_0 is the height of the vortices. The rotational velocity of the liquid in these vortices is maximum at the median depth and drops off to zero toward the top and bottom edges of the vortex. It is natural to assume that the atmospheric vortex in the Jovian Great Red Spot has approximately the same vertical structure—this is in fact assumed in the quasi-two-dimensional (baroclinic) soliton model of this natural vortex, studied in Sec. 5.1 (see the last footnote). Cyclonic vortices of this type (and their probable atmospheric analog—the Jovian Brown Ovals) are rarely encountered.

5.5. Alternative model of planetary vortices based on thermogyroconvection

An interesting model of global atmospheric vortices, differing radically from the one described above, was recently proposed by Hide and his coworkers.[121,122] We shall point out the basic idea, omitting the details (they would divert us from the subject of this review). In a liquid confined in the gap between two cylinders rotating around a vertical axis and having a horizontal bottom (i.e., in the absence of the β effect), a controllable radial temperature gradient, giving rise to a definite (small) density gradient, is created. This gradient, being noncollinear with the acceleration of gravity, creates in the liquid a flow (the so-called "thermal wind"[23,24,121,122]), directed along the azimuth.[32] If the gradient of the density (temperature) of the liquid at some location of the gap changes sign, then oppositely directed flows arise. These flows have either a cyclonic or anticyclonic curl, depending on the nature of the extremum of the density (maximum or minimum). Experiments[121,122] show that under certain conditions in such an arrangement the flows become unstable and generate chains of vortices with a different mode number. Under certain conditions, when the density of the liquid is minimum at the center of the gap (i.e.,

at a maximum of the temperature), the mode $m = 1$ appears: one anticyclone (in front of which, it is true, a weaker cyclone can be seen) fits into the perimeter of the system. Such a vortex structure is proposed in Refs. 121 and 122 as a model of the Jovian Great Red Spot. An extremum of the density with the opposite sign (maximum at the center of the gap) could not be created in the experiments of Refs. 121 and 122, and this situation was calculated numerically on a computer. According to the calculation, a cyclonic structure of the Jovian "barge" type should appear.

The model described differs very substantially from the soliton model presented above. The main differences are as follows. 1) The horizontal dimensions of the vortices in this model are significantly smaller than the depth of the liquid ("deep water"). Moreover, the effective height of the Jovian atmosphere ($H_0 \approx 25$ km) is three orders of magnitude smaller than the horizontal size of the JGRS. 2) The generated vortices are nondispersive (no β effect) and remain virtually stationary relative to the vessel. Therefore, the drift of the planetary vortices cannot be explained. 3) The observed cyclone-anticyclone asymmetry also cannot be explained. 4) In order to explain, based on this model, the properties of the JGRS vortex it is necessary to assume that the maximum temperature (minimum density) occurs at the center of the vortex, which qualitatively contradicts the observational data.[38,67] 5) The horizontal dimensions of the vortex are much smaller than the Rossby-Obukhov radius, and approximately equal the baroclinic (internal) Rossby radius r_i (see Sec. 1.4). This circumstance is similar to the conditions occurring in nature.

Some features of this model are similar to those of the soliton model studied above. First of all, the self-maintained vortex structure arises as a result of the instability of oppositely moving zonal flows (although the latter are created by different methods). Second, the dimensions of the vortices are physically comparable: they are determined by the Rossby scale, except that in the soliton model they are determined by the "two-dimensional" radius r_R while in Hide's model[122] they are determined by the "three-dimensional" radius r_i. It is possible that a new model of global planetary vortices, based on the synthesis of Hide's model and the soliton model, studied in this review, could appear as the development of the theoretical and experimental work proceeds.

6. POSSIBILITY OF THE EXISTENCE OF VORTEX STRUCTURES IN SPIRAL GALAXIES

Experimental data indicate the possibility in principle of the existence of vortex structures in the gaseous disks of spiral galaxies. These data were obtained in experiments[89–91,96,123a] on the modeling of the hydrodynamic mechanism[33] of generation of the spiral structure of galaxies using the "Spiral" experimental arrangement with differentially rotating shallow water. (The main elements of the arrangement (Fig. 22) are as follows: a rapidly rotating "core" consisting of a conical cup 8 cm in diameter (black color), a "tangential discontinuity" of the rotational velocity, and a less rapidly or relatively slowly rotating, in a particular case immobile, periphery; in the case a) the periphery is immobile and horizontal, while in the case b) it is a paraboloid rotating with a frequency $\Omega_2 = 0$, $2\Omega_1 = 3.6\ s^{-1}$, where $\Omega_1 = 18\ s^{-1}$ is the angular rotational frequency of the core.) The results of interest to us in this case consist in the fact that between the spiral surface density waves, generated by the hydrodynamic (centrifugal) instability, the disturbances of the liquid are of the nature of vortices shaped like bananas, strung onto the line of the velocity shear (Fig. 22b). The characteristic direction of rotation of these vortices is anticyclonic (opposite to the direction of rotation of the core), and in their drift motion around the core they lag behind the system of coordinates rotating with a velocity intermediate between the velocity of the core and the velocity of the periphery; in this coordinate system their radial dimensions are of the order of (and less than) the Rossby-Obukhov radius. Their amplitude is quite large: they turn out to be impenetrable to particles of the surrounding liquid.[34] The kinetic energy of the particles rotating in them approximately corresponds to the gravitational potential of the rise in the liquid in the spiral arms, as can be seen in Fig. 22b, where the particles of the vortices "ascend" onto the crests of the spirals and "slide" back down from them; it is possible that in the nonlinear regime of the centrifugal instability under study the vortices generate "ship waves" and thereby give rise to the buildup of the spiral arms.[89,90,123a] Thus the vortices and the spiral waves shown in Fig. 22 are elements of the same spiral-vortex structure generated by the hydrodynamic (centrifugal) instability of differentially rotating shallow

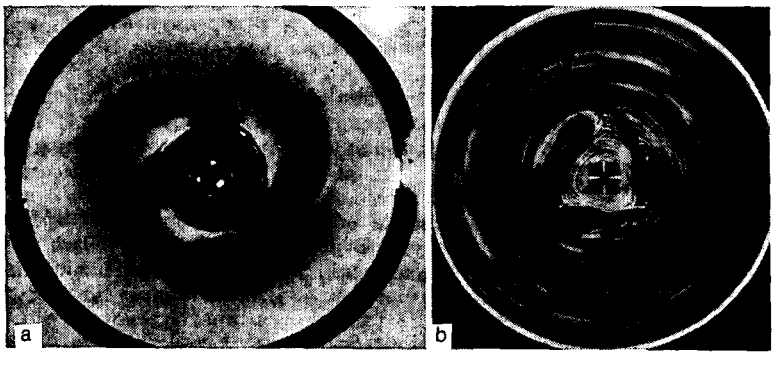

FIG. 22. a) Spiral surface density waves, excited in shallow water when the central "core" rotates more rapidly than the periphery.[89–91] Large-amplitude (white) vortices, effectively transporting particles of the liquid, can be seen at the base of the spirals, near the "discontinuity" in the rotational velocity. The "core" and the spiral waves rotate clockwise. b) Vortices in a system of spiral waves.[123a]

water (see Ref. 123a). It is important to note that the experiments performed[123a] satisfy the criterion of a "magnetized plasma": the visible length of the spiral arms and the radial size of the periphery are much larger[35] than the Rossby-Obukhov radius r_R, corresponding to the rotational frequency of the periphery $\Omega_2 = 0.2\Omega_1$; this criterion is fully compatible with the observed stability (steady-state behavior) of the spiral-vortex structure. [The vector nonlinearity apparently plays a significant role in the formation of this structure; see relation (15b).]

As already mentioned in Sec. 1.3, an important modification of the vector nonlinearity, associated with the dependence of the Rossby velocity (V_R) on the meridional coordinate y, and the "topographic" Rossby solitons generated by it, has been studied theoretically.[39] In Ref. 39 it is proposed that the change in V_R is caused by the presence of a meridional gradient of H, i.e., the depth of the liquid or the effective depth of the atmosphere (9). Such a gradient can be present in the gaseous disk of a galaxy, where the component of g normal to the plane of the disk drops off toward the periphery of the disk (edge effect). One can imagine in this case the formation (in the region of decreasing g) of structures of the Rossby soliton vortex type, "untwisted" by the instability of the differential rotation of the matter (gas) in the galaxy. The dimensions of these structures must, naturally, be of the order of several Rossby-Obukhov radii (8). In addition, they will be significantly smaller (at least severalfold) than the radial dimensions of the disk itself. Astronomical observations give some indications of the possibility of the existence of such vortex structures.[124–128] Their interpretation based on the above-studied particular solution for the Rossby soliton in the form of Ref. 55 is given in Ref. 57b.

7. INSTABILITY OF DIFFERENTIALLY ROTATING SHALLOW WATER AS A POSSIBLE UNIVERSAL MECHANISM OF GENERATION OF LARGE VORTICES ON LARGE PLANETS AND OF THE SPIRAL STRUCTURE OF GALAXIES WITH A JUMP IN THE VELOCITY ON THE ROTATION PROFILE

7.1. Alternation of the shear-flow instability modes (problem of the uniqueness of the JGRS vortex along the perimeter of the planet)

The instability of rotating shear flows is manifested in the most diverse situations and leads to the generation of chains of vortices of different nature: the anticyclonic solitons and Rossby cyclones described above, as well as vortices of a different nature.[110–112] Here a general behavior, expressed in the following two very distinct phenomena, is observed. The number of an azimuthal instability mode (m) (i.e., the number of vortices along the perimeter in a chain which is stationary in time) is related to the velocity u of (oppositely directed) shear flows[36] in a definite manner: 1) as u increases the number m decreases (see, for example, Figs. 17, 19, and 20); 2) *alternation* of modes is observed as u varies: for example, as $\bar{u}$ increases, the highest mode $(m+1)$ vanishes and the lowest mode m appears, etc., with the change in modes occurring in a discontinuous manner and exhibiting hysteresis—as u decreases, the inverse transition between a given pair of modes is observed at a lower value of u.

There are two instabilities which are characteristic of shear flows in the experiments under study on rotating shallow water[91]: the Kelvin-Helmholtz (KH) and centrifugal. We shall study the possible mechanism for the change in modes using the example of the better-studied KH instability.[37] This instability arises in the presence of a jump in the velocity at the boundary between flows irrespectively of which part of the liquid rotates faster—the center or the periphery. The increment of this instability can be written in the form

$$\gamma \approx \frac{\pi u}{\lambda}\left(1-\frac{5\delta}{\lambda}\right), \tag{49}$$

where λ is the wavelength, u is the jump in the velocity at the "discontinuity" between the flows, and δ is the width of the "discontinuity."[100,106] The threshold value of the jump in the velocity above which an instability appears can be estimated from the condition that the increment γ exceed the decrement d of viscous damping in shallow water: $d \approx \nu/H_0^2$, where ν is the kinematic viscosity and H_0 is the thickness of the layer of shallow water. From here we have

$$u_{cr} = \frac{\nu\lambda^2}{\pi H_0^2(\lambda-5\delta)}. \tag{50}$$

This is a well-known result: the instability exists only for $\lambda > 5\delta$.[100,106] It is evident that the modes closest to the shortest mode require a very high threshold and are therefore of no interest. Modes with $\lambda > 10\delta$ are more interesting. It is these modes that we shall have in mind. The increment of these modes, according to (49), increases as λ decreases (with weak spreading of the profile of the flows), and the higher is λ the less sensitive it is to an increase in δ. For this reason, as u increases, first of all, a "short-wavelength" mode appears—with a relatively large number of comparatively shallow vortices along the perimeter of the system. As u increases further, the obvious nonlinear evolution of this mode will cause δ to increase. In addition, a longer wavelength mode (with a smaller number of larger vortices along the perimeter) will begin to compete successfully with it—the increment of this mode, though smaller (with a weak smearing of the profile of the flows), is nevertheless less sensitive to δ. The development of this new mode will lead to an even larger increase in δ, as a result of which the preceding mode will vanish, etc. Thus the arising mode m suppresses the $(m+1)$ mode existing before it, and this amounts to a successive change of modes.

As regards the reasons for the natural vortex of the JGRS being the only one along the entire perimeter of the system, the mode-change behavior indicated above indicates that the mode $m = 1$ (one Rossby autosoliton along the perimeter of the system) exists with a zonal-flow profile that precludes the existence of the mode $m = 2$ (two autosolitons on the perimeter). For the mode $m = 2$ (corresponding to a shorter wavelength of the instability than in the case of the mode $m = 1$) this profile is too smooth: for it the indicated qualitative condition of the type $\lambda > 10\delta$ does not hold; in order for the mode $m = 2$ to arise, the profile must have a sharper velocity gradient along the meridian.

As the jump in the velocity between the oppositely moving flows decreases, the reverse transition from the given mode to a shorter wavelength mode will occur at a lower value of u than for the direct transition, because as the transition under study is approached from the side of large values of u the quantity δ is determined by the longer wavelength mode and therefore remains larger than when this transition is approached from the side of lower values of u, and this corresponds to the observed hysteresis.[88]

The second instability of shear flows is the centrifugal instability, which arises only when the center of the liquid rotates more rapidly than the periphery. In the linear theory of this instability[94] the following characteristics are pointed out: a) as the jump in the velocity of the flows increases, the increment of this mode increases and b) the longer wavelength mode is less sensitive to the width δ of the velocity jump. Based on this, one would think that the phenomenon of alternation of the modes of both instabilities is governed by a more or less common physical mechanism, associated with the action of analogous or close factors. (It is interesting to note that mode alternation, reminiscent of the behavior noted here, is also observed in the theory of stability of Rossby waves.[99])

7.2. Astrophysical applications

In Secs. 4 and 5 it was shown that large vortices in models of the atmospheres of large planets are generated as a result of the development of two instabilities: the Kelvin-Helmholtz (KH) instability and the centrifugal instability (CI), which are characteristic of zonal (oppositely directed) flows in a differentially rotating quasi-two-dimensional medium (liquid, gas). Under experimental conditions these instabilities can be quite easily distinguished, if the jump in the velocity u at the boundary between the flows is large enough compared with the characteristic velocity $c = (gH)^{1/2}$, which plays the role of an equivalent velocity of sound in (three-dimensionally) incompressible shallow water with a free surface.

Namely, if

$$u > 2\sqrt{2}c \qquad \left(\mathrm{Ma} \equiv \frac{u}{c} \gg 1\right), \tag{51}$$

when the effective (two-dimensional) compressibility of the medium plays the fundamental role, the two-dimensional KH instability is suppressed, as shown theoretically in Refs. 107 and 108 and experimentally in Ref. 84. In such fast flows instability (of the tangential shear) is manifested only as the centrifugal instability and develops only in the case when the interior parts of the liquid rotate more rapidly than the exterior parts, i.e., if the flows have an anticyclonic vorticity[82–88]; in other words, under conditions such that $\mathrm{Ma} \gg 1$ flows of the tangential shear type with a cyclonic vortex are stable, while those with an anticyclonic vortex are unstable, and in the latter case they generate vortex structures under one set of experimental conditions and spiral-vortex structures under different conditions.[89–91,123a] In this example we encounter the cyclone-anticyclone asymmetry in the *generation* of vortex structures with different sign of the vorticity, when, as in the case $\mathrm{Ma} < 1$, the asymmetry of the formation of cyclones and anticyclones is associated with the different degree of their steady-state behavior. A striking manifestation of the indicated asymmetry of cyclogenesis is the generation of a steady-state *anticyclonic* Rossby autosoliton (Sec. 4.6) in the mode $m = 1$ of the (apparently, centrifugal) instability. In this case the asymmetry is a result of both factors indicated above and is manifested in the fact that a *cyclonic* autosoliton (the only one along the perimeter of the system) does not exit.

The hydrodynamic instability of differentially rotating shallow water under study could be responsible for the generation of the spiral structure in the gaseous disks of galaxies, in which a jump in the rotational velocity occurs between the core and the periphery. This is indicated by model experiments[89–91,123a] (see also Ref. 96). In particular, the same sequence of azimuthal modes of the spiral structure as in the case of the generation of Rossby vortices is observed in them: in both cases, as the velocity jump at the "discontinuity" between the flows increases, a mode with a decreasing azimuthal wave number m, i.e., decreasing number of spiral arms and correspondingly decreasing number of vortices along the perimeter of the system (see also Ref. 123b), appears.

Thus the instability of differentially rotating shallow water with a free surface could be responsible for the formation of such different natural vortex structures as the large vortices in the atmospheres of large planets and the spiral pattern in galaxies with a velocity jump on the rotation profile.

8. DIPOLAR ROSSBY VORTICES (EXPERIMENT)

8.1. Formulation of the problem and the first experiments (small paraboloid)

A theoretical soliton structure in the form of a dipole or an isolated pair of cyclone-anticyclone vortices was described in Sec. 2.3.[51] The experimental search for such a structure was first initiated in Refs. 79 and 85 on a small paraboloid (see Table I above). The experiments performed gave essentially a negative result: they showed that although it is possible to generate a system of two coupled vortices with different signs,[79] the system is not of the dipolar soliton type.[51] This follows from the fact that the lifetime of the dipole pair, after which the constituent cyclone decays, is much shorter than that of a solitary (anticyclonic) Rossby soliton. In other words, under the conditions of the experiments of Refs. 79 and 85, for which a sharp cyclone-anticyclone asymmetry was characteristic (see, for example, Fig. 8 in Ref. 82), solitary ("monopolar") solitons were predominantly formed as a manifestation of the ("scalar") nonlinearity which predominates under the condition (15a), when the size of the vortex substantially exceeds the Rossby-Obukhov radius ($a > r_R$). This nonlinearity prevents the manifestation of the other ("vector") nonlinearity, which must predominate under the condition (15b), i.e., when $a < r_R$, and, according to the theory of Ref. 51, can form a paired (dipolar) Rossby soliton.

Based on the physical meaning of these two nonlinearities, of which one (the scalar nonlinearity) strongly depends

[illegible] variation in the depth of the liquid while the other (the vector nonlinearity) is less dependent on it, it was natural to assume that the competition between them could lead to a different result, if the depth of the liquid is significantly increased. But since in this case the radius r_R increases and the dimensions of the Rossby vortices increase correspondingly, in order that the radius of the vortex be much smaller than the radius of curvature of the vessel as before, the experiments have to be transferred from the small paraboloid to a large paraboloid (see Table I above). These experiments are described in the next section.

8.2. Experimental data (large paraboloid) and comparison with the theory

The experiments[96] on the larger experimental arrangement (the maximum diameter of the vessel equaled 70 cm; see Table I) were performed with a significantly larger depth of the liquid H_0: from 0.5 cm to 5 cm.

We shall first describe the results of experiments with a layer of liquid of moderate depth: $H_0 \lesssim 2.5$ cm. These experiments gave the following results. 1) They showed that there exists a simple and reliable method for generating a dipolar Rossby vortex, consisting of the following. The pumping disk (see Fig. 23) generates within ~ 5 s an extended cyclonic disturbance in the rotating paraboloidal layer of liquid, which can be thought of as being in the form of two oppositely directed flows. Soon after the disk is switched off, the flows excited by it generate two paired (dipolar) vortices. The two dipolar pairs formed in this manner move along the parallels in opposite directions and have at the same time the "appropriate" polarizations, corresponding to the relative motion of the vortex and the matter flowing around it. Namely, in a "westward" drifting pair (lagging behind the motion of the liquid as a whole), the outer vortex, located farther away from the center of the paraboloid, is a cyclone, while in an "eastward" drifting pair the outer vortex is an anticyclone. This result is shown in Fig. 23.[96] 2) The size of the dipolar vortices formed in this manner (the distance between the centers of the cyclone and anticyclone) $a \lesssim (1.5\text{–}2) r_R$. 3) The westward drift velocity of the dipolar vortices V_W is greater than the Rossby velocity: $V_W = 1.5\, V_R$. 4) The eastward drift velocity of the dipolar vortices is not known as accurately, but is close to the Rossby velocity: $V_E \approx 0.7\, V_R$. The properties 3) and 4) of these vortices are in good agreement with the theoretical relations (21). 5) The vortices move together with the trapped particles. 6) For the depth of the liquid under study (not large enough) the cyclone-anticyclone asymmetry is clearly observed in the paired vortices: the cyclone decays rapidly, and from the dipole only the anticyclone remains and exists for a comparatively long time (Figs. 23 and 24). This result can be explained by the predominance of the scalar nonlinearity. Under the indicated experimental conditions the paired vortices do not satisfy the condition (23), and they are therefore not solitons.

We shall now study the experiments with a large depth of the liquid: $H_0 \gtrsim 4$ cm. Under these conditions the cyclone-anticyclone asymmetry vanishes: the lifetime of the vortex

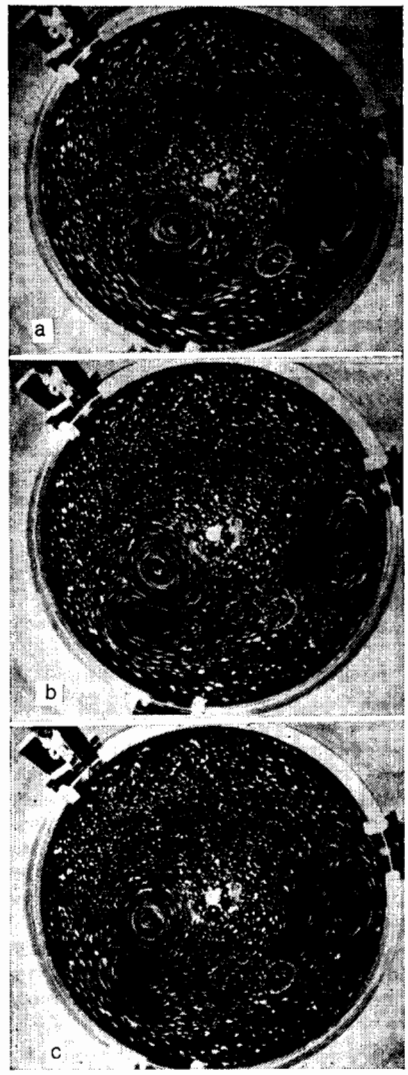

FIG. 23. Illustration of the method for creating two dipolar Rossby vortices with one pumping disk, rotating in the cyclonic direction in a time interval of ~ 5 s. The disk (lower right side of the photograph) generates an extended cyclonic disturbance, in which a bridge and two cyclones are formed (in the photograph they appear to be darker); then each cyclone forms an adjacent anticyclone and thus two dipoles are formed; in one of them, drifting clockwise ("westward"), the outer vortex (farther from the center of the vessel) is a cyclone, while in the other, drifting counterclockwise (eastward), the outer vortex is an anticyclone.

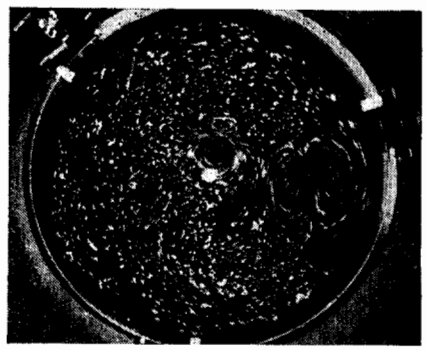

FIG. 24. Example of a dipolar Rossby vortex, created by the method shown in Fig. 23.[96] The pair of westward drifting vortices moves much more rapidly than its "nearest neighbor"—an eastward drifting pair. Large paraboloid, $H_0 = 2.5$ cm.

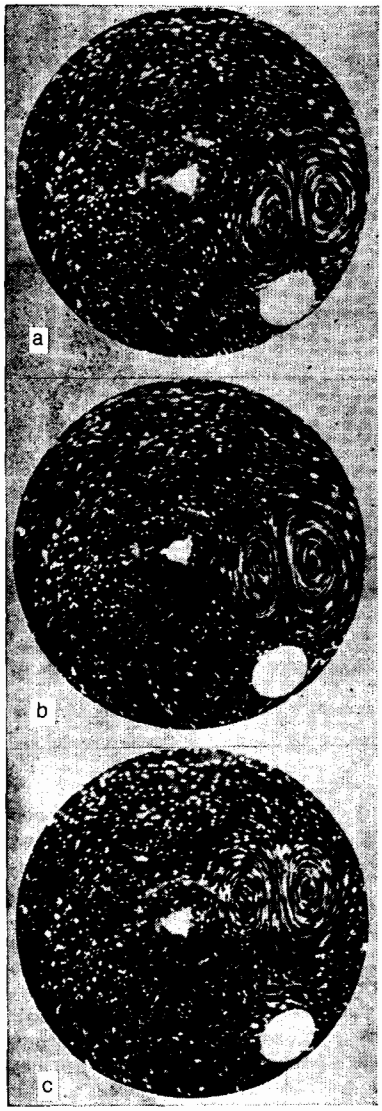

FIG. 25. Long-lived dipolar Rossby vortex drifting eastward. Large paraboloid, $H_0 = 4$ cm. The time intervals between the frames equal 2 and 8 s.

pair is no longer limited by the decay of the cyclone. This means that now the vector nonlinearity, forming mainly a dipolar vortex, predominates. The observed properties of this vortex (Fig. 25) are as follows: the maximum linear rotational velocity of the particles around the axis of the vortex on the profile equals about 10 cm/s, and it is approximately seven times higher than the drift velocity of the pair under the conditions of Fig. 25; the size of the vortex $a \approx (1.2\text{–}1.3) r_R$; the lifetime of the vortex is about 15–16 s, and this time is still shorter than the dispersion spreading time (24) of a linear packet of Rossby waves with the same dimensions: under the indicated conditions the dispersion time equals about 24 s. (Under the conditions of Fig. 25 the gradient of the depth of the liquid was oriented toward the center of the vessel; for this reason, the quantity V_R was less than and τ_L was greater than that indicated in Table I for the case $H = \text{const.}$) When the lifetime of the paired vortex is not limited by the decay of the cyclone, it can be limited by the separation of the partners (Fig. 26). This is apparently caused by the fact that the drift velocity is not constant over the size of the vortex and by the fact that the depth of the liquid in the cyclone is different from that in the anticyclone.

Thus, based on their dispersion properties or, which is the same thing, their propagation characteristics [the westward and eastward drift velocities satisfy the relations (21)], their dimensions [satisfying the condition (15b) for the vector nonlinearity to be the dominant nonlinearity], the trapping of particles of the medium, and their polarization, paired vortices, which are observed when the depth of the liquid is large enough, are very similar to the dipolar Rossby solitons described in the theory of Ref. 51 and formed by the vector nonlinearity. In order for these vortices to be confidently called solitons, their lifetime must be increased by a factor of at least two.

Vortices on rotating shallow water, in particular, paired vortices, were also observed in the experiments of Ref. 130, where they were called Rossby solitons. It should be noted,

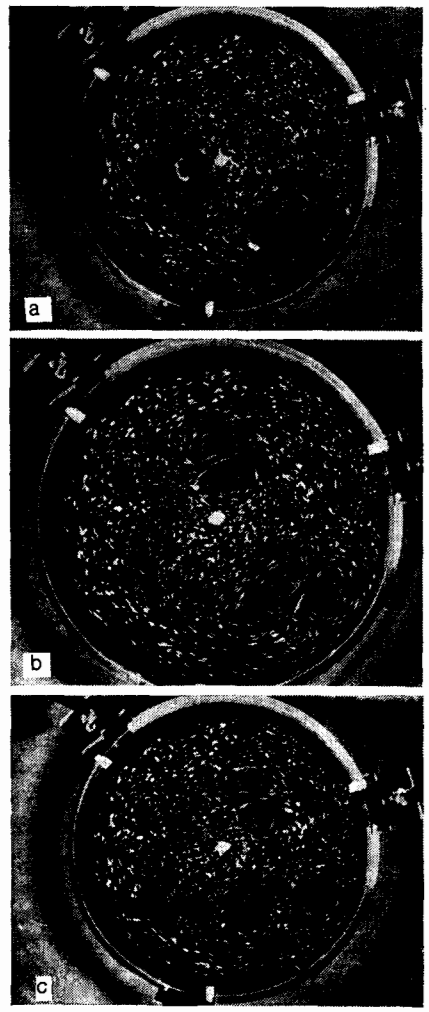

FIG. 26. Demonstration of the relatively rapid westward motion of the vortex pair.[96] In the dipolar westward drifting vortex the partners move away from one another. Large paraboloid, $H_0 = 2.5$ cm. The time intervals between the frames equal 8 and 7 s.

however, that the paraboloid used in the experiments of Ref. 130 had a very small slope (12 times smaller than that of the small paraboloid of Table I, and six times smaller than that of the large paraboloid in the same table), and therefore did not satisfy the conditions (23), (24), (34), (37), and (38), required for identifying vortices as Rossby solitons. Therefore the vortices observed in Ref. 130 cannot be identified as solitons—contrary to what is stated in Refs. 130 and 131.

Returning to the experiments, whose conditions satisfy the indicated necessary criteria, we recall that, as shown in Sec. 3.2.1, the anticyclonic Rossby soliton is an attractor. As regards paired Rossby vortices, when the depth of the liquid is relatively small ($H_0 \lesssim 2$ cm) they are not attractors, since the paired vortex—owing to the decay of the cyclone—transforms into an anticyclone, which is an attractor. As the depth of the liquid increases ($H_0 \gtrsim 4$ cm), however, the paired vortex already manifests definite properties of an attractor (they would be even more strongly manifested, if the partners of the vortex did not move away from one another).

There is another interesting fact that is observed in the experiments of Ref. 96 and characterizes, on the one hand, the cyclone-anticyclone asymmetry and, on the other, the collective properties of vortices (their interaction). The problem is that cyclogenesis by the method described above can, under certain conditions, produce not only two pairs, but an entire "chessboard" of vortices (Fig. 27). (In the theoretical study of Ref. 58 such a vortex ensemble, being hypothetical at the time, is called a Modon Sea.[38]) Thus the experiment (with a moderate depth of the liquid) shows that out of this entire "sea" after some time only anticyclones remain (!) (they are marked by arrows in Fig. 27); the cyclones decay.

The paired vortices described here differ substantially from the paired vortices formed in "deep water," as observed in the experiments of Ref. 132, under whose conditions there was no appreciable β effect.

The paired vortices observed in the experiments studied here are analogs of plasma vortices predicted theoretically in Refs. 133, 134, and 140–142.

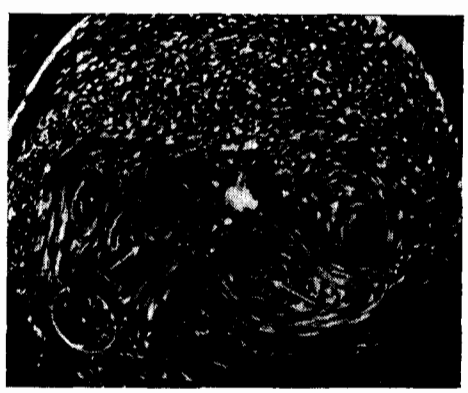

FIG. 27. Modon sea, from which after 5 s only anticyclones (marked by the arrows) remain in the form of vortices, while the cyclones decay; as a result, of six vortices only two remain (large paraboloid).[96]

CONCLUSIONS

So, Rossby solitons, observed experimentally in recent years (and Rossby vortices in general), are very interesting coherent nonlinear structures, which are probably directly related to large-scale planetary vortices and also possibly even to galactic vortices. The mechanism of their self-organization in zonal flows occurring in nature is quite general: it is related to the hydrodynamic instability of differentially rotating shallow water with a free surface—the instability which could be the basic mechanism for the formation of an autosoliton (JGRS) and the hydrodynamic mechanism for the generation of the spiral structure of galaxies. These are all examples of how an instability leads not to (small-scale) turbulence, but rather to the formation of large-scale quasi-two-dimensional structures.[39]

According to the theory, Rossby solitons (whose dimensions are greater than the Rossby-Obukhov radius) are the geophysical analog of drift solitons (whose dimensions are greater than the Larmor radius of ions) which can form in a nonuniform magnetized plasma and substantially affect its confinement time in magnetic traps (see, for example, Ref. 133 and also Ref. 134, where the concepts of dipolar solitons are transferred from hydrodynamics to plasma physics). Now that many of the properties and mechanisms of generation of Rossby solitons have been clarified in hydrodynamic experiments, it would be very interesting to carry out analogous experiments with drift (and related) solitons in a plasma. There are some indications that such solitons actually do exist. Indeed, looking back and thinking about the experiments performed approximately 20 years ago, it is logical to assume that the coherent structures observed under conditions of the drift instability[135] and the beam-drift instability[136–35] are probably close or physically analogous to the "drift" Rossby solitons studied in this review.

References 137–141 and the review in Ref. 142 can introduce the reader to the latest papers on the theory of drift nonlinear structures (in particular, solitons) and their possible effect on the nature of the motion of particles in a magnetized plasma. The belief (stated several years ago by B. B. Kadomtsev) that the existing experimental data on the spectra of low-frequency turbulence in plasma traps of the tokamak type can be explained based on the idea of a "gas" of drift solitons is developed theoretically in Ref. 137. The latter solitons, as indicated above, are analogous to Rossby solitons. Convective cells in plasmas are structurally similar to plasma vortices.[143–145]

The author thanks F. V. Dolzhanskiĭ and G. G. Sutyrin for carefully reading the manuscript, fruitful discussions, and suggestions.

[1)]In the English transcription—(J)GRS (Jovian Great Red Spot).

[2)]Theoretically these waves were known at the end of the last century[6] and were later studied in Ref. 8 (see the review of Ref. 9); modern observations of Rossby waves in the earth's atmosphere are described in Ref. 10a (see also Ref. 10b).

[3)]The term "autosoliton," in application to other specific structures, was first introduced by V. V. Osipov and B. S. Kerner; see Ref. 75 and the literature cited there.

[4)]In (9) k is the Boltzmann constant.

[5)]We recall that the propagation velocity of a Rossby soliton differs only by a nonlinear correction from the phase velocity of the linear wave as $\lambda \to \infty$.

[6)]The steep sections correspond to large wave numbers.

[7)]This argument is completely analogous to the conclusion drawn in Ref. 30 concerning the fact that on the "usual" branch of ion-acoustic waves (with negative dispersion) in a plasma a compression soliton is possible, while a rarefaction soliton is impossible. This also corresponds to the fact that the classical Scott Russell soliton in shallow water (the first soliton in the history of science)[28b] is a positive-elevation soliton (a solitary wave in the form of a depression is impossible in this case also). The solitons indicated here are solutions of the well-known Korteweig–de Vries equation (see Refs. 3a and 32).

[8)]These flows result from the evolution of the two-dimensional turbulence of the atmosphere[46]: small vortices coalesce, and in addition the increase in their scales along the parallels is not bounded, so that ring flows are formed; the increase of the scales along the meridian, however, is bounded by the Rhines length[114] $l \simeq \pi(u/\beta)^{1/2}$, where u is the amplitude of the flow velocity. As a result, zonal flows with a period of $\sim l$ are obtained (see Fig. 3).

[9)]The variant of Ref. 57a evidently has the same intrinsic feature as that of the variant of Ref. 55 studied below.

[10)]In plasma physics the scalar nonlinearity was studied earlier—in Ref. 59a (and later in Ref. 59b also): it was pointed out that a "scalar" drift-wave soliton can form in a spatially nonuniform magnetized plasma.

[11)]The trapping of particles of liquid by a monopolar Rossby soliton, the trapping condition ($V_{rot} > V_{dr}$) and the resulting new properties of Rossby solitons, in particular, their property of being attractors and the inelastic nature of their mutual collisions, were first discovered experimentally (Sec. 3.2), and they were taken into account in the theory under consideration only later.

[12)]The monopolar Rossby solitons studied above also have the property (21b).

[13)]The "vector" soliton is constructed based on this variability.[39]

[14)]With one exception, described in Sec. 3.3.

[15)]The formula (33) differs from Ref. 79 by a factor of 1/2 in the first term on the right side.[88]

[16)]The theorems for the existence and stability of Rossby solitons are proved precisely in this approximation; see, for example, Ref. 74.

[17)]This profile can be represented in the form $h = h_0 \exp(-r^2/2a_m^2$ or $h = h_0 \exp(-r^2/a^2)$, where $2a$ is the distance between diametrically opposite points on the profile, at which $h = h_0/e$.

[18)]In all photographs and figures presented the paraboloid rotates counterclockwise.

[19)]These experiments were performed in 1981 at the request of the participants of G. I. Barenblatt's seminar at the Institute of Oceanology of the USSR Academy of Sciences, and they are described in Refs. 79 and 82.

[20)]Or, which is the same thing, the region with closed streamlines.

[21)]Here there was no β effect: $\beta \simeq \partial(H/f)/\partial y = 0$.

[22)]The drift of Rossby solitons can be easily explained also on the basis of vortex representations.[82]

[23)]See, for example, Ref. 11.

[24)]The instability of the tangential velocity shear in a differentially rotating system has two modifications: the Kelvin-Helmholtz instability (KH) and the centrifugal instability (CI); see below.[91]

[25)]It is precisely this situation that is realized in the experiments and observations studied in this review.

[26)]The first threshold with a comparatively low flow velocity is apparently associated, as usual, with dissipation processes: viscosity and friction against the bottom.

[27)]The velocities of motions in planetary vortices are much lower than the velocity of sound, so that the medium may be regarded as incompressible; in this case the analogy between the behavior of these structures and that of shallow water is even more obvious.

[28)]According to what was said at the end of Sec. 2.2, the autosoliton described apparently is not directly related to the variant of the Rossby soliton in Ref. 55.

[29)]In real galaxies, generally speaking, both the centrifugal and Kelvin-Helmholtz instabilities can develop (see Ref. 123b for a more detailed discussion).

[30)]The quantity g' (physically less than g because of the effect of buoyancy) in this case is introduced as an adjustable parameter.

[31)]The details of the vertical structure of the JGRS (as yet not studied) cannot fundamentally alter the qualitative picture of the phenomenon presented.

[32)]This phenomenon is analogous to the drift of plasma particles in crossed electric and magnetic fields.

[33)]This mechanism has been investigated theoretically by A. M. Fridman and his coworkers starting in 1972 (see Refs. 89 and 90 for a discussion of this).

[34)]Unlike Rossby vortices, however, in the vortices described the centrifugal force from the characteristic rotation is no longer small compared to the Coriolis force (and even exceeds it), and the regime of the vortices is not the (geostrophic) Rossby regime (3). See Ref. 123a for a more detailed discussion.

[35)]For example, by an order of magnitude.

[36)]In the general case u is the jump in the velocity at the boundary between the flows.

[37)]For simplicity, we ignore the β effect.

[38)]The term "modon" is used (usually in the work of foreign authors) to denote different vortex structures, in particular, paired vortices.

[39)]As is evident from this review, experiment has played a decisive role in establishing these characteristics.

[1]a) H. J. Lugt, Vortex Flow in Nature and Technology, J. Wiley, New York, 1983; b) L. Bengtsson and J. Lighthill (Eds.), Intense Atmospheric Vortices, Springer-Verlag, N. Y., 1982 [Russ. transl., Mir, M., 1985].

[2]*G. B. Whitham, Linear and Nonlinear Waves, Wiley, Interscience, N. Y., 1974* [Russ. transl., Mir, M., 1977].

[3]a) B. B. Kadomtsev, Nelineĭnye yavleniya v plazme (Nonlinear Phenomena in Plasma), Nauka, M., 1979; b) B. B. Kadomtsev and V. I. Rydnik, Volny vokrug nas (Waves Around Us), Znanie, M., 1981.

[4]a) M. J. Lighthill, Waves in Fluids, Cambridge University Press, N. Y., 1978 [Russ. transl., Mir, M., 1981]; b) H. P. Greenspan, The Theory of Rotating Fluids, Cambridge University Press, N. Y., 1968 [Russ. transl., Gidrometeoizdat, L., 1975].

[5]M. Van Dyke, An Album of Fluid Motion, Parabolic Press, Stanford (1982).

[6]M. Margules, Sitzungber, Akad. Wiss. Wien. **102**, 11 (1893); S. S. Hough, Philos. Trans. R. Soc. London A **189**, 201 (1897); **191**, 139 (1898).

[7]C. G. Rossby, J. Marine Res. **2**, 38 (1939).

[8]B. Haurwitz, Gerl. Beitr. Geophys. **51** (1937); J. Marine Res. **3**, 254 (1940); E. N. Blinova, Dokl. Akad. Nauk SSSR **39**, 285 (1943).

[9]G. W. Platzman, Quart. J. Meteor. Roy. Soc. **94**, 225 (1968).

[10]a) R. A. Madden, Rev. Geophys. Space Phys. **17**, 1935 (1979); b) D. Andrews, Nature **310**, 185 (1984).

[11]E. B. Gledzer, F. V. Dolzhanskiĭ, and A. M. Obukhov, Sistemy gidrodinamicheskogo tipa i ikh primenenie (Systems of Hydrodynamic Type and Their Application), Nauka, M., 1981, p. 130; A. M. Obukhov, G. S. Golitsyn, and F. V. Dolzhanskiĭ, Nekotorye problemy sovremennoĭ fiziki atmosfery (Some Problems in the Modern Physics of the Atmosphere), Nauka, M., 1981, p. 94.

[12]F. V. Dolzhanskiĭ and G. S. Golitsyn, Izv. Akad. Nauk SSSR, Fiz. Atmos. Okeana **13**, 795 (1977) [Izv. Atm. Ocean. Phys. **13**, 550 (1977)].

[13]N. A. Phillips, Tellus **17**, 295 (1965).

[14]A. Ibbetson and N. A. Phillips, Tellus **19**, 81 (1967).

[15]J. R. Holton, Geophys. Fluid Dynamics **2**, 323 (1971).

[16]F. V. Dolzhanskiĭ, M. V. Kurganskiĭ, and Yu. L. Chernous'ko, Izv. Akad. Nauk SSSR. Fiz. Atmos. Okeana **15**, 597 (1979); Yu. L. Chernous'ko, *ibid.*, 1048 [Izv. Atm. Ocean. Phys. **15**, 408 (1979)].

[17]J. R. Holton, An introduction to dynamic meteorology, Academic Press, N. Y., 1976 [Russ. transl., Gidrometeoizdat, Leningrad, 1976].

[18]A. M. Obukhov, M. V. Kurganskiĭ, and M. S. Tatarskaya, Meteor. Gidrol., No. 10, 5 (1984) [Sov. Meteor. Hydrol. No. 10, 1 (1984)].

[19]a) V. M. Kamenkovich, M. N. Koshlyakov, and A. S. Monin, Sinoptícheskie vikhri v okeane (Synoptic Vortices in the Ocean), Gidrometeoizdat, L., 1982, Sec. 2.3; b) M. N. Koshlyakov and A. S. Monin, Vikhri v okeane. Nauka i chelovechestvo (Vortices in the Ocean: Science and Man), Znanie, M., 1985, p. 87.

[20]A. R. Robinson [Ed.], Eddies in Marine Sciences, Springer-Verlag, New York (1983).

[21]E. N. Parker, Astrophys. J. **162**, 665 (1970).

[22]P. A. Gilman, Science **160**, 760 (1968); A. S. Monin, Usp. Fiz. Nauk **132**, 123 (1980) [Sov. Phys. Usp. **23**, 594 (1980)].

[23]P. H. Le Blond and L. A. Mysak, Waves in the Ocean, Elsevier, New York, 1978 [Russ. transl., Mir, M., 1981].

[24]J. Pedlosky, Geophysical Fluid Dynamics, Springer-Verlag, N. Y., 1982 [Russ. transl., Mir, M., 1984].

[25]N. E. Kochin, I. A. Kibel', and N. V. Roze, Teoreticheskaya gidromekhanika (Theoretical Hydrodynamics), Fizmatgiz, M., 1963.

[26]a) V. M. Kamenkovich and G. M. Reznik, Gidrodinamika okeana (Hydrodynamics of the Ocean), edited by V. M. Kamenkovich and A. S. Monin, Nauka, M. (1978), Chapter 7; b) V. M. Kamenkovich and A. S. Monin, *ibid.*, Chapter 1.
[27]L. M. Brekhovskikh and V. V. Goncharov, Vvedenie v mekhaniku sploshnykh sred (Introduction to the Mechanics of Continuous Media), Nauka, M., 1982.
[28]a) N. J. Zabusky and M. D. Kruskal, Phys. Rev. Lett. **15**, 240 (1965); b) E. Scott, Volny v aktivnykh i nelineĭnykh sredakh v prilozhenii k élektronike (Waves in Active and Nonlinear Media in Application to Electronics), Sov. radio, M., 1977, Supplement I; c) F. Calogero and A. Degasperis, Spectral Transforms and Solitons, North Holland, N. Y., 1982 [Russ transl., Mir, M., 1985]; d) R. K. Bullough and P. J. Caudrey (Eds.), Solitons, Springer-Verlag, Berlin, 1980 [Russ. transl., Mir, M., 1983]; e) J. L. Lamb, Vvedenie v teoriyu solitonov (Introduction to the Theory of Solitons), Mir, M., 1983.
[29]a) V. E. Zakharov, S. V. Manakov, S. P. Novikov, and L. P. Pitaevskiĭ, Teoriya solitonov (Theory of Solitons), Nauka, M., 1980; b) V. I. Karpman, Nelineĭnye volny v dispergiruyushchikh sredakh, Nauka, M., 1973 [Engl. transl., Nonlinear Waves in Dispersive Media, Pergamon Press, Oxford, 1975]. c) K. E. Lonngren and A. Scott (Eds.), Solitons in Action, Academic Press, N.Y., 1978 [Russ. transl., Mir, M., 1981].
[30]A. A. Vedenov, E. P. Velikhov, and R. Z. Sagdeev, Yad. Sintez, **1**, 82 (1961).
[31]R. Z. Sagdeev, Voprosy teorii plazmy (Problems in Plasma Theory), edited by M. A. Leontovich, Atomizdat, M., 1964, Vol. 4, p. 20.
[32]B. B. Kadomtsev and V. I. Karpman, Usp. Fiz. Nauk **103**, 193 (1971) [Sov. Phys. Usp. **14**, 40 (1971/1972)].
[33]K. Lonngren, Plasma Phys. **25**, 943 (1983); Y. Nakamura, IEEE Trans. **PS-10**, 180 (1972).
[34]L. M. Degtyarev, V. G. Makhan'kov, and L. I. Rudakov, Zh. Eksp. Teor. Fiz. **67**, 533 (1974) [Sov. Phys. JETP **40**, 264 (1974)].
[35]M. V. Nezlin, Dinamika puchkov v plazme (Dynamics of Beams in Plasmas), Énergoizdat, M., 1982.
[36]B. A. Smith and G. Hunt, Jupiter, ed. T. Gehrels, University of Arizona Press, Tucson, 1976 [Russ. transl., Mir, M., 1979, Vol. 2, p. 433].
[37]G. Hunt and P. Moore, Jupiter, Rand McNally, Chicago, 1981.
[38]a) B. A. Smith, R. A. Soderblom, T. V. Johnson *et al.*, Science **204**, 951 (1979); b) E. J. Reese and B. A. Smith, Icarus **9**, 474 (1968).
[39]P. M. Rizzoli, Adv. Geophys. **24**, 147 (1983); P. M. Rizzoli and M. C. Hendershott, Dynam. Atmos. Oceans **4**, 247 (1980).
[40]Ya. B. Zel'dovich, A. V. Mamaev, and S. F. Shandarin, Usp. Fiz. Nauk **139**, 153 (1983) [Sov. Phys. Usp. **26**, 77 (1983)].
[41]J. G. Charney and G. R. Flierl, Evolution of Physical Oceanography, eds. B. A. Warren and C. Wunsch, MIT Press, Cambridge, 1981.
[42]a) G. P. Williams and T. Yamagata, J. Atmos. Sci. **41**, 453 (1984); b) G. P. Williams, *ibid.* **42**, 1237 (1985); c) T. Matsuura and T. Yamagata, J. Phys. Oceanogr. **12**, 440 (1982).
[43]D. L. T. Anderson and P. D. Kilworth, Deep Sea Res. **26**, 1033 (1979).
[44]M. V. Nezlin, Pis'ma Astron. Zh. **10**, 530 (1984) [Sov. Astron. Lett. **10**, 221 (1984)].
[45]A. Hasegawa, S. G. Maclennan, and Y. Kodama, Phys. Fluids **22**, 2122 (1979).
[46]A. Hasegawa, Adv. Phys. **34**, 1 (1985).
[47]R. R. Long, J. Atmos. Sci. **21**, 197 (1964); D. J. Benney, J. Math. Phys. **45**, 52 (1966); A. Clarke, Geophys. Fluid. Dyn. **2**, 343 (1971).
[48]M. E. Stern, J. Marine Res. **33**, 1 (1975).
[49]L. G. Redekopp, J. Fluid Mech. **82**, 725 (1977); T. Maxworthy and L. G. Redekopp, Icarus **29**, 281 (1976); Science **210**, 1350 (1980).
[50]a) R. Hide, Nature **190**, 895 (1961); b) A. P. Ingersoll, Science **182**, 1346 (1973).
[51]V. D. Larichev and G. M. Reznik, Dokl. Akad. Nauk SSSR **231**, 1077 (1976).
[52]G. R. Flierl, V. D. Larichev, J. C. McWilliams, and G. M. Reznik, Dynam. Atmos. Oceans **5**, 1 (1980).
[53]G. R. Flierl, *ibid.* **3**, 15 (1979).
[54]É. N. Mikhaĭlova and N. B. Shapiro, Izv. Akad. Nauk SSSR, Fiz. Atmos. Okeana **16**, 823 (1980) [Izv. Atm. Ocean. Phys. **16**, 587 (1980)].
[55]V. I. Petviashvili, Pis'ma Zh. Eksp. Teor. Fiz. **32**, 632 (1980) [JETP Lett. **32**, 619 (1980)].
[56]R. Z. Sagdeev, V. D. Shapiro, and V. I. Shevchenko, Pis'ma Astron. Zh. **7**, 505 (1981) [Sov. Astron. Lett. **7**, 279 (1981)].
[57]a) V. I. Petviashvili, *ibid.* **9**, 253 (1983) [Sov. Astron. Lett. **9**, 137 (1983)]; b) V. I. Korchagin and V. I. Petviashvili, *ibid.* **11**, 298 (1985) [Sov. Astron. Lett. **11**, 121 (1985)].
[58]A. S. Volokitin and V. V. Krasnosel'skikh, Dokl. Akad. Nauk SSSR **260**, 588 (1981) [Sov. Phys. Dokl. **26**, 863 (1981)].
[59]a) V. N. Oraevsky, H. Tasso, and H. Wobig, Plasma Physics and Controlled Nuclear Fusion Research, IAEA, Vienna (1969), Vol. 1, p. 671; b) V. I. Petviashvili, Fiz. Plazmy **3**, 270 (1977) [Sov. J. Plasma Phys. **3**, 150 (1977)].
[60]M. V. Nezlin, Pis'ma Zh. Eksp. Teor. Fiz. **34**, 83 (1981) [JETP Lett. **34**, 77 (1981)].
[61]A. P. Ingersoll and D. Pollard, Icarus **52**, 62 (1982); A. P. Ingersoll and P. G. Cuong, J. Atmos. Sci. **38**, 2067 (1981); A. P. Ingersoll, Sci. Amer. **245**(6), 66 (1981).
[62]P. J. Conrath, P. J. Gierarsch, and N. Nath, Icarus **48**, 256 (1981).
[63]E. J. Reese and B. A. Smith, Icarus **9**, 474 (1968).
[64]V. R. Eshleman, G. L. Tyler, G. E. Wood *et al.*, Science **206**, 959 (1979).
[65]T. Oven and R. J. Terille, J. Geophys. Res. A **86**, 8797 (1981).
[66]C. W. Hord, R. A. West, K. E. Simmons *et al.*, Science **206**, 956 (1979).
[67]R. Hanel, B. Conrath, M. Flasar *et al.*, *ibid.* **204**, 972.
[68]A. Hatzes, D. D. Wenkert, A. P. Ingersoll, and G. E. Danielson, J. Geophys. Res. A **86**, 8745 (1981).
[69]B. A. Smith, R. Soderholm, R. Batson *et al.*, Science **215**, 504 (1982).
[70]N. N. Romanova and V. Yu. Tseitlin, Izv. Akad. Nauk SSSR, Fiz. Atmos. Okeana **20**, 115 (1984). Izv. Atm. Ocean Fiz. **20**, 85 (1984)].
[71]H. Lamb, Hydrodynamics, Dover Publications, N. Y., 1945 [Russ. transl., Gostekhizdat, M., 1947].
[72]G. K. Batchelor, Introduction to Fluid Dynamics, Cambridge University Press, N. Y., 1967 [Russ. transl., Mir, M., 1973].
[73]G. G. Sutyrin, a) Dokl. Akad. Nauk SSSR **280**, 1101 (1985); b) Izv. Akad. Nauk SSSR, Ser. Mekhanika Zhidkosti i Gaza **4**, 119 (1985).
[74]Yu. A. Danilov and V. I. Petviashvili, Itogi nauki i tekhniki, Ser. Fizika plazmy (Progress in Science and Technology, Series in Plasma Physics), edited by V. D. Shafranov, VINITI, M., 1983, No. 4, p. 5.
[75]V. V. Osipov and B. S. Kerner, Zh. Eksp. Teor. Fiz. **89**, 589 (1985) [Sov. Phys. JETP **62**, 337 (1985)].
[76]a) A. V. Gaponov-Grekhov and M. I. Rabinovich, Fizika XX veka (Physics of the 20th Century), Nauka, M., 1984, p. 219; b) Nelineĭnye volny (Nonlinear Waves), edited by A. V. Gaponov-Grekhov and M. I. Rabinovich, Nauka, M., 1983; c) Self-Organization: Autowaves and Structures Far from Equilibrium, edited by V. I. Krinsky, Springer-Verlag, New York (1984); d) I. Prigogine, From Being to Becoming, W. H. Freeman, San Francisco, 1980 (Russ. transl., Nauka, M., 1985]; e) H. Haken (ed.), Synergetics, Springer-Verlag, N.Y., 1977 [Russ. transl., Mir, M., 1985].
[77]M. I. Rabinovich and D. I. Trubetskov, Vvedenie v teoriyu kolebaniĭ i voln (Introduction to the Theory of Oscillations and Waves), Nauka, M., 1984.
[78]S. V. Antipov, M. V. Nezlin, E. N. Snezhkin, and A. S. Trubnikov, Pis'ma Zh. Eksp. Teor. Fiz. **33**, 368 (1981) [JETP Lett. **33**, 351 (1981)].
[79]S. V. Antipov, M. V. Nezlin, E. N. Snezhkin, and A. S. Trubnikov, Zh. Eksp. Teor. Fiz. **82**, 145 (1982) [Sov. Phys. JETP **55**, 85 (1982)].
[80]S. V. Antipov, M. V. Nezlin, V. K. Rodionov, E. N. Snezhkin, and A. S. Trubnikov, Pis'ma Zh. Eksp. Teor. Fiz. **35**, 521 (1982) [JETP Lett. **35**, 645 (1982)].
[81]S. V. Antipov, M. V. Nezlin, V. K. Rodionov, E. N. Snezhkin, and A. S. Trubnikov, Pis'ma Astron. Zh. **9**, 58 (1983) [Sov. Astron. Lett. **9**, 32 (1983)].
[82]S. V. Antipov, M. V. Nezlin, V. K. Rodionov, E. N. Snezhkin, and A. S. Trubnikov, Zh. Eksp. Teor. Fiz. **84**, 1357 (1983) [Sov. Phys. JETP **57**, 786 (1983)].
[83]M. V. Nezlin, E. N. Snezhkin, and A. S. Trubnikov, Pis'ma Zh. Eksp. Teor. Fiz. **36**, 190 (1982) [JETP Lett. **36**, 234 (1982)].
[84]S. V. Antipov, M. V. Nezlin, V. K. Rodionov, E. N. Snezhkin, and A. S. Trubnikov, *ibid.* **37**, 319 (1983) [JETP Lett. **37**, 378 (1983)].
[85]S. V. Antipov, M. V. Nezlin, V. K. Rodionov, E. N. Snezhkin, and A. S. Trubnikov in Ref. 76b, p. 87.
[86]S. V. Antipov, M. V. Nezlin, E. N. Snezhkin, and A. S. Trubnikov, Proceedings of the 2nd International Workshop on Nonlinear and Turbulent Processes in Physics, Kiev-83, Gordon and Breach, New York (1984), p. 665.
[87]S. V. Antipov, M. V. Nezlin, and A. S. Trubnikov, Pis'ma Zh. Eksp. Teor. Fiz. **41**, 25 (1985) [JETP Lett. **41**, 30 (1985)].
[88]S. V. Antipov, M. V. Nezlin, E. N. Snezhkin, and A. S. Trubnikov, Zh. Eksp. Teor. Fiz. **89**, 1905 (1985) [Sov. Phys. JETP **62**, 1097 (1985)].
[89]A. G. Morozov, M. V. Nezlin, E. N. Snezhkin, and A. M. Fridman, Pis'ma Zh. Eksp. Teor. Fiz. **39**, 504 (1984) [JETP Lett. **39**, 613 (1984)].
[90]A. G. Morozov, M. V. Nezlin, E. N. Snezhkin, and A. M. Fridman,

Usp. Fiz. Nauk **145**, 160 (1985) [Sov. Phys. Usp. **28**, 101 (1985)].
[91]A. M. Fridman, A. G. Morozov, M. V. Nezlin, and E. N. Snezhkin, Phys. Lett. A **109**, 228 (1985).
[92]V. L. Polyachenko and A. M. Fridman, Ravnovesie i ustoĭchivost' gravitiruyushchikh sistem (Equilibrium and Stability of Gravitating Systems), Nauka, M. (1976).
[93]A. M. Fridman and V. L. Polyachenko, Physics of Gravitating Systems, Springer-Verlag, New York, 1984, Vol. 1, 2.
[94]A. G. Morozov, Pis'ma Astron. Zh. **3**, 195 (1977) [Sov. Astron. Lett. **3**, 103 (1977)]; Astron. Zh. **56**, 498 (1979) [Sov. Astron. **23**, 278 (1979)].
[95]G. R. Flierl, J. Phys. Oceanogr. **7**, 365 (1977).
[96]M. V. Nezlin and E. N. Snezhkin, Lectures at the 7th All-Union School on Nonlinear Waves, Gor'kiĭ, March 1985; Nelineĭnye volny (Nonlinear Waves) (ed.) A. V. Gaponov-Grekhov and M. I. Rabinovich, Nauka, M., 1986.
[97]B. B. Kadomtsev and A. I. Ryazanov, Priroda., No. 8, 2 (1983).
[98]G. G. Sutyrin and I. G. Yushina, Dokl. Akad. Nauk SSSR **288**, 585 (1986).
[99]F. V. Dolzhanskiĭ, Izv. Akad. Nauk SSSR. Fiz. Atmos. Okeana **21**, 383 (1985) [Izv. Atm. Ocean. Phys. **21**, 292 (1985)].
[100]Lord Rayleigh, Theory of Sound, Dover Publications, N. Y., 1945 [Russ. transl., Gostekhizdat, M., 1955, Ch. 21].
[101]L. D. Landau and E. M. Lifshitz, Gidrodinamika, Nauka, M., 1986 [Engl. transl. of earlier ed. Fluid Mechanics, Pergamon Press, London (1959).
[102]A. V. Timofeev, Usp. Fiz. Nauk **102**, 185 (1970) [Sov. Phys. Usp. **13**, 632 (1971)].
[103]L. A. Dikiĭ, Gidrodinamicheskaya ustoĭchivost' i dinamika atomosfery (Hydrodynamic Stability and Dynamics of the Atmosphere), Gidrometeoizdat, L., 1976.
[104]S. A. Maslou, in Hydrodynamic Instabilities and Transition to Turbulence (Eds.), H. Swiney and J. Gollub, Springer-Verlag, N. Y., 1985, Chap. 7 [Russ. transl., 1st ed., Mir, M., 1984].
[105]P. Ripa, J. Fluid Mech. **126**, 463 (1983).
[106]Ya. B. Zel'dovich and P. I. Kolykhalov, Dokl. Akad. Nauk SSSR **266**, 302 (1982) [Sov. Phys. Dokl. **27**, 699 (1982)].
[107]L. D. Landau, Dokl. Akad. Nauk SSSR **44**, 151 (1944).
[108]S. V. Bazdenkov and O. P. Pogutse, Pis'ma Zh. Eksp. Teor. Fiz. **37**, 317 (1983) [JETP Lett. **37**, 375 (1983)].
[109]A. B. Mikhaĭlovskiĭ, V. R. Kudashev, V. P. Lakhin, L. A. Mikhailovskaya, A. I. Smolyakov, and S. Yu. Shishkov, *ibid.* **40**, 273 (1984) [JETP Lett. **40**, 1054 (1984)].
[110]M. Rabaud and Y. Couder, J. Fluid Mech. **136**, 291 (1983).
[111]F. V. Dolzhanskiĭ, Izv. Akad. Nauk SSSR, Fiz. Atmos. Okeana **17**, 563 (1981) [Izv. Atm. Ocean. Phys. **17**, 413 (1981)].
[112]Yu. L. Chernous'ko, *ibid.* **16**, 423 (1980) [Izv. Atmos. Ocean. Phys. **16**, 285 (1980)].
[113]D. J. Tritton and P. A. Davis in: Ref. 104, Chapter 8.
[114]P. B. Rhines, J. Fluid Mech. **69**, 417 (1975); Ann. Rev. Fluid Mech. **11**, 401 (1979).
[115]G. P. Williams, J. Atmos. Sci. **36**, 932 (1979).
[116]G. S. Golitsyn, Icarus **13**, 1 (1970).
[117]M. Allison and P. H. Stone, Icarus **54**, 296 (1983).
[118]D. Nof, J. Phys. Oceanogr. **11**, 1662 (1981); J. Marine Res. **40**, 57 (1982).
[119]J. P. Dugan, R. P. Mied, P. C. Mignerey, and A. F. Schuetz, J. Geophys. Res. C **87**, 385 (1982).
[120]P. D. Killworth, J. Phys. Oceanogr. **13**, 368 (1983).
[121]P. L. Read and R. Hide, Nature **302**, 126 (1983).
[122]P. L. Read and R. Hide, Nature **308**, 45 (1984).
[123]a) M. V. Nezlin, V. L. Polyachenko, E. N. Snezhkin, A. S. Trubnikov, and A. M. Fridman, Pis'ma Astron. Zh. **12**, 504 (1986) [Sov. Astron. Lett. **12**, No. 4 (1986)]; b) A. G. Morozov, M. V. Nezlin, E. N. Snezhkin, Yu. M. Torgashin, and A. M. Gridman, Astron. Tsirk., No. 1414, 1, 4, 7 (1986).
[124]A. V. Zasov and G. A. Kyazumov, Pis'ma Astron. Zh. **7**, 131 (1981) [Sov. Astron. Lett. 7, 73 (1981)].
[125]V. L. Afanas'ev and S. S. Rassokhin, *ibid.* **8**, 515 (1982) [Sov. Astron. Lett. **8**, 277 (1982)].
[126]B.T. Lunds, Astrophys. J. **28**, 391 (1974).
[127]G. Tenorio-Tagle, Astron. Astrophys. **88**, 61 (1980).
[128]R. Hayward, Publ. Astron. Soc. Pacif. **76**, 35 (1964).
[129]A. V. Khutoretskiĭ, Izv. Akad. Nauk SSSR, Fiz. Atmos. Okeana **22**, 344 (1986).
[130]R. A. Antonova, V. P. Zhvaniya, D. G. Lominadze, D. I. Nanobashvili, and V. I. Petviashvili, Pis'ma Zh. Eksp. Teor. Fiz. **37**, 545 (1983) [JETP Lett. **37**, 651 (1983)].
[131]V. I. Petviashvili and V. V. Yan'kov, Voprosy teorii plazmy (Problems in Plasma Theory), Energoatomizdat, M. (1985), Vol. 14, p. 3.
[132]G. R. Flierl, M. E. Stern, and J. A. Whitehead, Dyn. Atm. Oceans **7**, 233 (1983).
[133]K. Nozaki, Phys. Rev. Lett. **46**, 184 (1981).
[134]M. Makino, T. Kamimura, and T. Sato, J. Phys. Soc. Japan **50**, 954 (1981).
[135]N. S. Buchel'nikova, R. A. Salimov, and Yu. I. Éĭdel'man, Zh. Eksp. Teor. Fiz. **52**, 837 (1967) [Sov. Phys. JETP **25**, 548 (1967)].
[136]M. V. Nezlin, M. I. Taktakishvili, and A. S. Trubnikov, Zh. Eksp. Teor. Fiz. **55**, 397 (1968) [Sov. Phys. JETP **28**, 208 (1969)]; M. V. Nezlin and A. M. Solitsev, Zh. Eksp. Teor. Fiz. **48**, 1237 (1965) [Sov. Phys. JETP **21**, 826 (1965)].
[137]J. D. Meiss and W. Horton, Phys. Fluids **25**, 1838 (1982); **26**, 990 (1983).
[138]P. K. Shukla, Phys. Scr. **32**, 141 (1985).
[139]P. C. Liever, Nucl. Fusion **25**, 543 (1985).
[140]E. W. Laedke and K. H. Spatschek, Phys. Fluids **28**, 1008 (1985).
[141]P. K. Shukla, M. Y. Yu, and R. K. Warms, *ibid.*, 1719.
[142]A. B. Mikhaĭlovskiĭ, Nonlinear Phenomena in Plasma and Hydrodynamics (ed.), R. Z. Sagdeev, Mir, M., 1986.
[143]R. Z. Sagdeev, V. D. Shapiro, and V.I. Shevchenko, Fiz. Plazmy **4**, 555 (1978) [*sic*].
[144]P. K. Shukla, M. Y. Yu, H. U. Rahman, and K. H. Spatschek, Phys. Rept. **105**, 227 (1984).
[145]H. L. Pecseli, Y. Rasmussen, and K.Thomsen, Phys. Rev. Lett. **52**, 2148 (1984); Plasma Phys. **27**, 837 (1985).

Translated by M. E. Alferieff